ANALYSIS OF STATISTICAL PARAMETERS DERIVED FROM SATELLITE DIGITAL DATA (JULY 1978 GOES-WEST) FOR USE IN DIAGNOSING MARINE FOG AREAS.

Otto Frank McNab

NAVAL POSTGRADUATE SCHOOL
Monterey, California

THESIS

ANALYSIS OF STATISTICAL PARAMETERS DERIVED FROM SATELLITE DIGITAL DATA (JULY 1978 GOES-WEST) FOR USE IN DIAGNOSING MARINE FOG AREAS

by

Otto Frank McNab

March 1979

Thesis Advisor: R. J. Renard

Approved for public release; distribution unlimited.

SECURITY CLASSIFICATION OF THIS PAGE (When Data Entered)

REPORT DOCUMENTATION PAGE

READ INSTRUCTIONS BEFORE COMPLETING FORM

1. REPORT NUMBER	2. GOVT ACCESSION NO.
3. RECIPIENT'S CATALOG NUMBER	
4. TITLE (and Subtitle) Analysis of Statistical Parameters Derived from Satellite Digital Data (July 1978 GOES-West) for Use in Diagnosing Marine Fog Areas	5. TYPE OF REPORT & PERIOD COVERED Master's Thesis; March 1979
	6. PERFORMING ORG. REPORT NUMBER
7. AUTHOR(s) Otto Frank McNab	8. CONTRACT OR GRANT NUMBER(s)
9. PERFORMING ORGANIZATION NAME AND ADDRESS Naval Postgraduate School Monterey, California 93940	10. PROGRAM ELEMENT, PROJECT, TASK AREA & WORK UNIT NUMBERS
11. CONTROLLING OFFICE NAME AND ADDRESS Naval Postgraduate School Monterey, California 93940	12. REPORT DATE March 1979
	13. NUMBER OF PAGES 68
14. MONITORING AGENCY NAME & ADDRESS(if different from Controlling Office)	15. SECURITY CLASS. (of this report) Unclassified
	15a. DECLASSIFICATION/DOWNGRADING SCHEDULE

16. DISTRIBUTION STATEMENT (of this Report)

Approved for public release; distribution unlimited.

17. DISTRIBUTION STATEMENT (of the abstract entered in Block 20, if different from Report)

18. SUPPLEMENTARY NOTES

19. KEY WORDS (Continue on reverse side if necessary and identify by block number)

20. ABSTRACT (Continue on reverse side if necessary and identify by block number)

GOES West Infrared (IR) and Visual (VIS) satellite observations for the North Pacific Ocean area, 35-55N, 120W-180°, at 2345 GMT for eight June/July 1978 dates are processed to yield 20 statistical parameters which are analyzed for their use in discerning the existence of marine fog. The exploratory sample of 522 satellite observations, at 3 nmi x 3 nmi resolution (at subsatellite point) are related to the associated 0000 GMT synoptic ship reports which serve the role of ground truth. The

DD FORM 1 JAN 73 1473 EDITION OF 1 NOV 65 IS OBSOLETE
S/N 0102-014-6601 |
(Page 1)

SECURITY CLASSIFICATION OF THIS PAGE (When Data Entered)

best discrimination between fog/no-fog observations, using the statistical parameters, occurs for stratification of the data by the meridional component of the wind (south vs north), IR temperature ($\geq$ 269 K vs < 269 K) and the standard deviation of IR temperature ($\leq$ 2 K vs > 2 K).

Approved for public release; distribution unlimited.

Analysis of Statistical Parameters Derived from Satellite Digital Data (July 1978 GOES-West) for Use in Diagnosing Marine Fog Areas

by

Otto Frank McNab
Lieutenant, United States Navy
B.S., Centenary College of Louisiana, 1971

Submitted in partial fulfillment of the
requirements for the degree of

MASTER OF SCIENCE IN METEOROLOGY AND OCEANOGRAPHY

from the

NAVAL POSTGRADUATE SCHOOL

March 1979

ABSTRACT

GOES West Infrared (IR) and Visual (VIS) satellite observations for the North Pacific Ocean area, 35-55N, 120W-180°, at 2345 GMT for eight June/July 1978 dates are processed to yield 20 statistical parameters which are analyzed for their use in discerning the existence of marine fog. The exploratory sample of 522 satellite observations, at 3 nmi x 3 nmi resolution (at subsatellite point) are related to the associated 0000 GMT synoptic ship reports which serve the role of ground truth. The best discrimination between fog/no-fog observations, using the statistical parameters, occurs for stratification of the data by the meridional component of the wind (south vs north), IR temperature ($\geq$ 269 K vs $<$ 269 K) and the standard deviation of IR temperature ($\leq$ 2 K vs $>$ 2 K).

TABLE OF CONTENTS

LIST OF TABLES

LIST OF FIGURES

ACKNOWLEDGEMENTS

The author would like to express his deep appreciation to Dr. Robert J. Renard, without whose patient guidance and assistance the completion of this study would not have been realized.

Special thanks are extended to Ms. Pimeron Zeleney, Naval Environmental Prediction Research Facility (NEPRF) and to Mr. Richard Daley, Space Science and Engineering Center (SSEC), University of Wisconsin, Madison, Wisconsin for their assistance in adapting the SSEC navigation software for use at the Naval Postgraduate School (NPS). Also special thanks to Mr. Mike McDermet and the personnel assigned to the Meteorology Laboratory, NPS, for their attention to the technical needs of the author.

Appreciation is also extended to the Fleet Numerical Weather Central (FNWC), Monterey, California, for providing the synoptic ship observations used in the study; to the personnel at the SSEC, particularly Mr. Tom Haig, Mr. Fred Mosher, and Mr. J. T. Young who were of assistance in furnishing and advising on the use of GOES West data and training on the McIDAS; to the National Environmental Satellite Service (NESS), Redwood City, California, for providing GOES West satellite imagery; and to the NESS, Washington, D.C., particularly to Dr. Henry Fleming and his associates in providing technical advice on evaluating digital geostationary satellite data.

Also, many special thanks are extended to my adorable wife, who endured many lonely nights which the author spent at the NPS computer center.

I. INTRODUCTION AND BACKGROUND

Ship accidents due to reduced visibility because of fog exact a heavy toll in materiel and human life (Quayle, 1976). For the Navy, marine fog curtails carrier flight operations as well as surface craft operations. A study over a five-year period concerning dollar cost and, more importantly losses of human life, emphasizes the impact of marine fog upon naval operations (Wheeler, 1974).

Accurate diagnosis and prognosis of marine fog regions over the open ocean would reduce the type of casualties referred to above and enhance the capability of any naval operation in which the limiting parameter is horizontal visibility. A specific application of fog prognosis is in Optimum-Track Ship Routing (OTSR), a program in existence at Fleet Numerical Weather Central, Monterey, California (FNWC).

The only operational objective hemispheric fog forecasts generated on a daily basis are those produced by the FNWC for all areas of the Northern Hemisphere. Their product, called FTER, is a computerized probability of advective fog, and is promulgated twice daily at 0000 and 1200 GMT for forecast intervals up to 72 hours. These fog forecasts are statistically derived from numerical model output parameters (U.S. Naval Weather Service Command, 1975).

Observations by meteorological satellites may be useful in improving the diagnosis of marine fog areas and concomitant increases in forecast accuracy. Research conducted at the Naval Postgraduate School, Monterey, California (NPS), in 1974 and 1975, utilized visual (VIS) and infrared (IR) weather satellite imagery from polar-orbiting satellites to qualitatively diagnose the presence of marine fog over the North Pacific Ocean. Initial

results indicated that further investigation into the use of digital satellite data for determining marine fog was necessary (Wallace and Renard, 1975). Using NOAA-2 digital satellite data, continuing investigations in 1975 established optimal ranges of digital count values (DCV's), or gray shades, for fog occurrence for both VIS and IR data (Hale and Renard, 1975). The level of skill achieved in applying these findings indicated that further research was necessary. Research conducted in 1976 and 1977 was directed to the feasibility of using VIS and IR digital data from both the military polar-orbiting meteorological satellite, Defense Meteorological Satellite Program (DMSP) Satellite, and the Synchronous Meteorological Satellite (SMS-2), as recorded over the eastern North Pacific Ocean area (Ihli and Renard, 1977). Optimal VIS and IR ranges for the occurrence of marine fog were determined for SMS-2, while the DMSP data set was too limited for meaningful analysis. The results obtained in this study were promising enough to warrant a more extensive test using Geostationary Operational Environmental Satellite (GOES) data. Such a study was initiated in fall 1978 utilizing GOES West June/July 1978 digital data from the eastern North Pacific Ocean.

II. OBJECTIVES AND APPROACH

The immediate objective of the subject research is to identify physical statistical parameters derivable from VIS and IR weather satellite observations which may be used to discriminate ocean areas of marine fog from areas where no fog exists. The ultimate objective is to combine such parameters with numerically-derived model output parameters in a regression scheme to specify fog areas at initial time and yield a persistence factor useful in prognostic time. The numerical statistical aspect of the research has been on-going since 1977 (Van Orman and Renard, 1977; Quinn, 1978).

The approach utilized to pursue the immediate objective was to study various statistical distributions of parameters dependent on temperature and reflected radiance as observed by radiometric sensing in the IR and VIS channels, respectively, of the North Pacific Ocean GOES-West satellite. Related statistical approaches were utilized by the Inter-American Tropical Tuna Commission (Stevenson, Kirkham and Madsen, 1977) to screen clouds for sea-surface temperature diagnosis and by the University of Maryland (Booth, 1973) for objective cloud type classification. These research endeavors provided important background for this study.

Data from polar-orbiting satellites, such as DMSP, were not considered here, in part due to the experience of the previous researchers (Ihli and Renard, 1977). The GOES has the advantage of taking observations at short intervals and hence can be readily matched in time to ground truth synoptic observations.

III. DATA

A. AREA OF STUDY

The area of study was limited to that portion of the eastern North Pacific Ocean within the following boundaries: 35-55N; 120W-170E (Figure 1). The area selected was a compromise due to several factors: the coverage provided by the GOES-West satellite; data storage constraints imposed by the Space Science and Engineering Center, University of Wisconsin, Madison, Wisconsin (SSEC), where the data were received; and the climatological area of marine fog occurrence (Figure 1).

B. PERIOD OF STUDY AND GROUND-TRUTH DATA

July, climatologically speaking, records the most frequent occurrence of marine fog over the North Pacific Ocean (U.S. Navy, Naval Oceanography and Meteorology, 1978). Thus it was arranged to have GOES West observations recorded at the SSEC for the period starting with 0245 GMT 27 June 1978 and ending with 2345 GMT 4 August 1978. Specifically, VIS and IR digital data were retrieved daily for 0245, 1745, 2045 and 2345 GMT with certain exceptions (Table I). The exceptions were due in part to the navigational parameters being unavailable for all times during this period, and machine and operator error. The amount of data actually used was a subset of 8 days between 27 June and 13 July 1978. This period was selected since the operational satellite was transferred to a stand-by mode while replacing it with a new vehicle in the 14-16 July time period. Thus, it appeared that a sufficient exploratory sample was available for study. The possibility of greater variance in the satellite parameters due to combining data from two satellites was thus avoided.

The 0000 GMT primary synoptic observation time only was selected for study since all longitudes under study were in daylight at that time (1600 LST at 120W to 1100 LST at 165E) and VIS as well as IR data (at 2345 GMT) could be considered. The surface ship weather observations which provided "ground truth" were obtained from FNWC. These observations were classified into one of 41 fog likelihood categories (FLC) (following Willms, 1975) which were further combined into seven FLC Groups (FLCG) and finally three divisions (FLCGD) (Tables II, III). This was accomplished for the 1001 ship reports. After considering all of the fog cases (FLCG 1-6) (Figure 2) and selecting only those corresponding non-fog cases (FLCG7) in the same general vicinity, the number of ship reports was reduced to 522, or approximately 52% of the original data.

C. GOES WEST DATA

GOES West digital data were furnished on magnetic tape by the SSEC in their save tape format, a means of recording many data frames onto a single magnetic tape. The dynamic range of both the VIS and IR sensors is 0 to 255 (NASA, 1976). Low (high) DCV values for VIS data correspond to surfaces having low (high) albedo, while low (high) DCV values for IR data indicate relatively high (low) temperatures.

The Visible and Infrared Spin Scan Radiometer (VISSR) aboard GOES West scans in the west/east direction on each spin of the spacecraft. In the visible region (0.55-0.75 micrometers) VISSR scans eight parallel lines on each spin, providing about 1 km (0.5 nmi) resolution, while in the infrared (10.5-12.6 micrometers) VISSR scans one line on each spin, providing roughly 8 km (4 nmi) resolution at nadir (NOAA, NASA, 1976). These line to line resolutions deteriorate as the field of view (FOV)

moves further away from the subpoint (Figure 3). Along each scan line the data resolution is nominally 1 km (0.5 nmi) for VIS data and 4 km (2 nmi) for IR data at the subsatellite point (equator at 135W), with less deterioration than the line to line resolution at points removed from nadir.

Since ship positions are recorded to tenths of degrees and since areas of marine fog were deemed to be quite extensive, it was decided that a 3 nmi x 3 nmi pixel size would be sufficient for the processing of the digital satellite data thereby reducing the quantity of data from that available and minimizing the ensuing cost of processing. The 3 nmi VIS data are obtained by averaging successively every six samples (each sample at half nmi intervals) along a line, placing the result at the fourth sample position. In the case of IR where every other line is redundant information, every third element and line are moved by one mile where elements and lines are at 2 nmi intervals (Figure 4).

IV. DATA ANALYSIS AND RESULTS

A. APPROACH

The approach adopted was to compute 20 statistical parameters for both the VIS and IR observations (Appendix A, after Booth, 1973) at and in the vicinity of the locations of the 522 0000 GMT ground-truth synoptic ship reports and to compare the average values for each of seven FLCG's. These 7 FLCG's were combined into 3 divisions (Tables II, III) in order to have a minimal number of related groups, thereby allowing a sufficient number of ship observations to be included in each division so as to give statistical meaning to the parameter values.

B. GOES-WEST DATA ANALYSIS

Satellite orbital elements necessary to earth locate the satellite observations were provided by the SSEC. These were received in final usable form at the NPS in early January 1979. Prior to this time, during a five-day period at the SSEC in August 1978, five days of the ground truth synoptic ship report data were located in satellite coordinates (line, pixel) by the author. The process of retrieving line and element positions for each ship observation position on the McIDAS Interactive Computer at the SSEC proved to be inefficient for the author's purposes and only provided the location of the ship report in each data frame time (i.e., time of receipt of satellite observations). This process disallowed further efficient use of the VIS and IR data sets for each frame time and thus did not contribute to the computation of the 20 statistical parameters. Moreover, it was discovered in late CY78 that an incomplete set of navigational parameters was available from the SSEC. Fortunately,

the satellite division at the Naval Environmental Prediction Research Facility, Monterey, California (NEPRF) was provided with the SSEC software for earth locating the satellite data, thus it became more expedient to perform the navigational processing at the NPS for all of the satellite data. Ship position (latitude and longitude), total cloud cover, low cloud cover and type, height of low cloud base, middle and high cloud types, surface wind direction and speed, FLC, and FLCG, along with the satellite frame time, were coded as inputs to the analysis program.

Both the VIS and IR GOES-West digital satellite data were checked on each of the eight days for the distribution of DCV's in the range 0-255. Due to data processing at NESS, "holes" or zerocounts appeared methodically in the distribution of IR DCV's (Figure 5). However, this problem was rectified by converting DCV-values into equivalent black-body temperatures according to

$$T(K) = \begin{cases} 330 - \frac{DCV}{2} , & DCV \leq 176 \\ \\ 418 - DCV , & DCV > 176 \end{cases}$$

This conversion was done before statistically manipulating the data to derive the 20 statistical parameters. This problem was not exhibited by the VIS data.

Further, in the IR data a temperature of 330 K occasionally occurred. Such a datum was considered an indicator of missing or erroneous data, thus invalidating the usefulness of the particular array of satellite data surrounding a ground-truth point. Also, since the temperature range 300-330 K has no meteorological significance in the area of study, IR DCV

values between 0 and 60 are suspect. A similar statement is true for the temperature range 198-163 K (IR DCV values between 220 and 255). Therefore any non-zero DCV in either of the above ranges may be attributable to signal processing noise of the GOES-West satellite digital data.

Next the ship position was located inside the data frame in both the VIS and IR data. Initially, an area approximately 84 x 90 nmi at 45N, 160W (16 lines x 32 pixels) surrounding the ship location was extracted from the data frame, and the statistical parameters computed for both IR and VIS data. This area size appeared to be too large, especially for a FOV near 55N, 160W (i.e., 119 x 105 nmi). The area size was reduced to 8 lines by 16 pixels, which is approximately 42 x 45 nmi at 45N, 160W, and 60 x 52 nmi at 55N, 160W. This decision was not entirely arbitrary since a compromise between an area of sufficient size to justify statistical averaging and yet small enough to be representative of events at the ground-truth point was necessary. Considered to be a partial justification for the size selected is the fact that the averages of the array mean temperatures and of the array mean albedos were not very different from the averages of the temperatures and of the albedos located at the ship position.

Having computed the 20 parameters for each observation point, scatter diagrams were used to compare the VIS and IR parameters in order to determine some discrimination between fog (FLCG1) and no-fog (FLCG7). There appeared to be little success here. (For example compare Figure 6(a) and 6(b).) These early efforts were largely motivated by the need to separate cases of low cloud only (with or without fog) from cases "contaminated" by middle and/or high cloud. With this in mind a stratification of cases according to average IR temperature cut-offs of 260 K and

269 K was investigated. The 260 K cut-off was abandoned after showing little evidence of being able to achieve discrimination of fog/no fog cases. The 269 K cut-off appeared to be a more likely discriminator, at least in principle, since 700 kPa climatological temperatures indicate this to be a reasonable low value across the study area of the North Pacific Ocean (Figure 7), and thus a suitable minimum for tops of low clouds. Moreover, the distributions of fog/no fog cases from the limited sample are nearly equal.

Next the 269 K mean IR temperature was combined with the standard deviation of temperature, $S \gtrless 2$ K, as a trial discriminator of fog/no fog cases (Figure 8). Thus, statistics for the following array mean temperature and standard deviation ($\bar{T}$, $\bar{S}_T$) categories were tabulated for the ground-truth synoptic ship report locations: all $\bar{T}$; $\bar{T} \geq 269$ K; $\bar{T} \geq 269$ K with $S_T \leq 2$ K; $\bar{T} \geq 269$ K with $S_T > 2$ K; $\bar{T} < 269$ K; $\bar{T} < 269$ K with $S_T \leq 2$ K; and $\bar{T} < 269$ K with $S_T > 2$ K (Table IV). At this point there appears to be little discrimination between fog/no fog divisions I, II, III for each temperature/standard deviation stratification. Of course there are differences in the values of the statistical parameters from one temperature/standard deviation category to another but this is to a large measure merely evidence of expected variation due to differences between middle/high-cloud contaminated cases ($\bar{T} < 269$ K) and mostly low-cloud arrays ($\bar{T} \geq 269$ K), and in part due to variable cloud type in each stratification (as stratified vs cumuliform clouds).

The next step was to stratify the sample by cloud cover (N), a variable contained in the synoptic report at each ground-truth location. It was reasoned that some veiling of discrimination between fog/no fog was due to variable sky cover and hence variable $\bar{T}$, S, gradient, etc. Simply,

the reports were separated by $N \geq .8$ and $N < .8$ with statistics shown for the former (Table V). Unfortunately, the sample is considerably reduced, but this is mostly due to elimination of no-fog cases and the attendant partially cloudy skies; the effect is considered positive. In this test there appears to be increased fog discrimination among the parameters, more specifically between FLCG1 and FLCG7. However, the sample for $\bar{T} < 269$ K with $S_T \leq 2$ K is too small to be considered significant for this analysis.

The test was repeated using N_h as a discriminator, where $N_h \leq N$. As before, the reports were separated by $N_h \geq .8$ and $N_h < .8$ with statistics shown for the former (Table VI).

Previous work in the Department of Meteorology, NPS (Renard and Servaas, 1977; Van Orman and Renard, 1977) indicated the value of wind direction as a discriminator of fog/no-fog. Thus, the satellite data were further processed to relate the IR and VIS samples to ground-truth observations with $N_h \geq .8$ and south (100° to 270°) or north (280° to 090°) winds (calm cases were omitted). The best results to date were obtained in this segment of the study (Tables VII, VIII). In order to focus on the increasing parameter discrimination of fog/no fog cases with each enhanced stratification step (Tables V-VIII), the parameter differences Division I (FLCG1) - Division III (FLCG7) were computed and are presented in Table IX. It is obvious from the table that the best division of fog (FLCG1)/no fog (FLCG7) occurs with $\bar{T} \geq 269$ K and $S_T \leq 2$ K for south and north wind segments. For example, without the aid of any of the 20 statistical parameters, for $\bar{T} \geq 269$ K, $S_T \leq 2$ K and south winds, no fog (FLCG7) occurs only 23% of the time while north winds are associated with no fog 62% of the time. The results are similarly

definite for $\bar{T} \geq 269$ K, $S_T > 2$ K and south winds, but the sample is too small to be significant. In any case, the statistical parameter differences Div I versus Div III also maximize for these groups, especially in the VIS observation, thus allowing for further modulation of these empirical probabilities based on a processing of the differences.

The final experiment was conducted to increase the fog (Div I) sample by allowing FLCG2 to be combined with FLCG1, since FLCG2 observations are, in general, fog at observation time, although light. Table X shows the differences (Div I_M(FLCG1,2) - Div III (FLCG7)) for the same categories as Table IX south and north wind discrimination samples only. Comparing the values of Tables IX and X, the advantage of combining FLCG1 and 2 appears questionable and this facet of the research was not pursued further at this time.

V. CONCLUSIONS AND RECOMMENDATIONS

The principal objective of this study was to identify physical statistical parameters derivable from VIS and IR weather satellite-observations which may be used to discriminate ocean areas of marine fog from areas where no fog exists. Through the interpretation and processing of digital GOES-West satellite data using conventional surface ship reports as ground-truth verification, a surface report possessing a mean temperature ($\bar{T}$) greater than or equal to 269 K, a standard deviation of temperature (S_T) less than or equal to 2 K, and a south wind component has a relatively high frequency of fog for $N_h \geq .8$. Also for north winds having the same temperature characteristics, no fog has a relatively high frequency. Further, the differences in mean statistical parameter values between fog/no-fog cases tend to maximize especially for VIS observations, given south-component winds, $\bar{T} \geq 269$ K, $S_T \leq 2$ K, $N_h \geq .8$. To a lesser extent this statement is also true for north-component winds, all other conditions the same. Beyond this, lack of a sufficiently large sample precludes definite conclusions.

Though the size of the sample is small, important hints as to the usefulness of GOES West in indicating marine fog areas are evident. Therefore, the following recommendations are offered for future studies:

(1) Conduct a similar study utilizing at least the remaining 16 days of 2345 GMT GOES-West satellite digital data.

(2) Compute kurtosis values for the VIS DCV and IR temperature distributions as a twenty-second parameter.

(3) Further examine statistical relationships between conventional synoptic ship report data and both VIS DCV and IR temperature distributions.

(4) Utilize the linear regression approach to test the significance of those satellite parameters (predictors) apparently contributing to specifying the probability of fog/no fog.

(5) Vary the stratification IR temperature and standard deviation temperature values to maximize the differences in mean parameter values between fog/no-fog cases.

APPENDIX A: PARAMETER COMPUTATIONS

Each set of 8 x 16 IR and VIS satellite observations centered on the ground-truth 0000 GMT synoptic ship report is treated as a one-dimensional array of 128 values in computing the following parameters (refer to Appendix B for parameter listing).

The mean is computed by:

$$m = \frac{1}{n}\sum_{i=1}^{n} X_i \qquad (n=128) \qquad \text{Parameter 1}$$

where X_i is the observed value.

The second and third moments about the mean are computed by the following formula:

$$u_k = \frac{1}{n}\sum_{i=1}^{n} (X_i - m)^k \quad \text{for } k=2\&3 \ .$$

Values of the standard deviation (S), coefficient of variation (CV), and skewness (SK) are computed by the following formulae:

$$S = \sqrt{\frac{nu_2}{n-1}} \qquad \text{Parameter 3}$$

$$CV = S/m \qquad \text{Parameter 4}$$

and

$$SK = u_3/(u_2\sqrt{u_2}) \qquad \text{Parameter 5}$$

Values at 1, 16, 50, 84 and 99% cumulative frequencies (CF) are determined (Parameters 6-10) with the range defined as:

$$\text{range (R)} = 99\%\ \text{CF} - 1\%\ \text{CF} . \qquad \text{Parameter 11}$$

Parameter 12 is the median minus the mean.

The next six parameters (Parameters 13-18) are computed by considering the following element configuration:

$$\begin{array}{ccc} & A & \\ & \uparrow & \\ & \Delta x & \\ & \downarrow & \\ D & E - B & ; \quad \Delta x = 1 \text{ unit}, \\ & C & \end{array}$$

where the gradient (G) and Laplacian (L) are computed by

$$G = \left[\frac{1}{4}(B-D)^2 + \frac{1}{4}(C-A)^2\right]^{\frac{1}{2}}$$

and

$$L = A + B + C + D - 4E .$$

The minimum and maximum are algebraically selected for both G and L, and the arithmetic mean values for both are computed in the usual sense.

The power spectrum is computed by transforming each set of 8 x 16 observations f(I,J) into the spatial frequency domain F(μ,v) by using a two-dimensional fast Fourier transform (FFT). The transformed observation is then normalized by multiplying by its complex conjugate $F^*(\mu,v)$:

$$C(\mu,v) = F^*(\mu,v) \cdot F(\mu,v) .$$

The power spectrum parameters (P) (Parameters 19-21) are computed by combining row and column variances centered about the two-dimensional plane at wavenumber i:

$$P(i) = \sum_{\mu=-i}^{i} \sum_{v=-i}^{i} C(\mu,v) - \sum_{\mu=-j}^{j} \sum_{v=-j}^{j} C(\mu,v) \quad \text{for } i=1,2,3.$$

The power spectrum parameters are normalized so that

$$\sum_{i=1}^{3} P(i) = 1.0 \ .$$

APPENDIX B: LIST OF GOES-WEST WEATHER SATELLITE PARAMETERS AND THEIR SYMBOLIZATIONS WITH UNITS

Legend: $\bar{Y}(\bar{\bar{Y}})$ indicates average of a number of single array values (single array mean values)

Parameters	Symbols	Units
1. Temperature (VIS DCV)	$\bar{\bar{T}}(\bar{\bar{A}})$	K(DCV)
2. Station Temperature (VIS DCV)	$\bar{T}_{STA}(\bar{A}_{STA})$	K(DCV)
3. Standard deviation of temperature (VIS DCV)	$\overline{S_T}(\overline{S_A})$	K(DCV)
4. Coefficient of variation of temperature (VIS DCV)	$\overline{CV_T}(\overline{CV_A})$	None
5. Temperature (VIS DCV) skewness	$\overline{SK_T}(\overline{SK_A})$	"
6. 1% cumulative frequency of temperature (VIS DCV)	$\overline{CFT_{1\%}}(\overline{CFA_{1\%}})$	K(DCV)
7. 16% " "	$\overline{CFT_{16\%}}(\overline{CFA_{16\%}})$	"
8. 50% " "	$\overline{CFT_{50\%}}(\overline{CFA_{50\%}})$	"
9. 84% " "	$\overline{CFT_{84\%}}(\overline{CFA_{84\%}})$	"
10. 99% " "	$\overline{CFT_{99\%}}(\overline{CFA_{99\%}})$	"
11. Temperature (VIS DCV) range	$\bar{R}_T(\bar{R}_A)$	"
12. Temperature (VIS DCV) median-mean	$\bar{M}_T(\bar{M}_A)$	"
13. Temperature (VIS DCV) gradient	$\bar{\bar{G}}_T(\bar{\bar{G}}_A)$	$K/2\Delta x$ $(DCV/2\Delta x)$
14. Minimum temperature (VIS DCV) gradient	$\bar{G}_{MIN_T}(\bar{G}_{MIN_A})$	"
15. Maximum temperature (VIS DCV) gradient	$\bar{G}_{MAX_T}(\bar{G}_{MAX_A})$	"
16. Laplacian (VIS DCV) gradient	$\bar{\bar{L}}_T(\bar{\bar{L}}_A)$	K(DCV)
17. Algebraic minimum temperature (VIS DCV) Laplacian	$\bar{L}_{MIN_T}(\bar{L}_{MIN_A})$	"

18.	Algebraic maximum temperature (VIS DCV) Laplacian	$\bar{L}_{MAX_T}$ ($\bar{L}_{MAX_A}$)	K(DCV)
19.	Normalized power spectrum variance of temperature (VIS DCV): wavenumber 1	$\overline{\overline{P_T}}^1$ ($\overline{\overline{P_A}}^1$)	% of total variance
20.	Normalized power spectrum variance of temperature (VIS DCV): wavenumber 2	$\overline{\overline{P_T}}^2$ ($\overline{\overline{P_A}}^2$)	"
21.	Normalized power spectrum variance of temperature (VIS DCV): wavenumber 3	$\overline{\overline{P_T}}^3$ ($\overline{\overline{P_A}}^3$)	"

TABLE I. Available GOES-West satellite navigational parameters as a function of time (GMT) for study period.

x indicates gamma values available for picture time
-- indicates gamma values missing for picture time

Date	2:45	17:45	20:45	23:45
27 June 1978	x	x	x	x
28	x	x	x	x
29	x	--	x	--
30	--	x	x	x
1 July	x	x	x	x
2	x	x	x	x
3	--	--	--	--
4	x	x	x	x
5	x	x	x	x
6	--	x	x	--
7	--	--	x	--
8	--	x	x	--
9	--	--	--	--
10	--	x	x	--
11	--	x	--	--
12	--	x	--	--
13	--	--	x	x
14	x	x	x	x
15	--	x	x	x
16	--	--	--	--
17	--	x	--	--
18	--	x	x	x
19	x	x	x	x
20	--	x	x	x
21	--	--	x	x
22	x	x	x	x
23	x	x	x	x
24	x	x	x	x
25	x	x	x	x
26	x	x	x	x
27	x	x	x	x
28	x	x	--	x
29	--	x	x	x
30	--	--	--	--
31	--	x	x	x
1 August	--	--	--	--
2	--	--	--	--
3	--	x	x	--
4	--	x	x	x

TABLE II. Marine-fog likelihood categories (FLC) as dependent on the visibility-weather group elements of the primary synoptic report.

Fog Likelihood Categories	Coded Visibility	Coded Present Weather	Coded Past Weather
1	*	40-49	4
2	*	40-49	5
3	*	10	4
4	*	11,12	4
5	*	10	5
6	*	11,12	5
7	90-93	**	4
8	90-93	H	4
9	94	**	4
10	94	H	4
11	90-93	**	5
12	90-93	H	5
13	94	**	5
14	94	H	5
15	*	28	4
16	*	28	5,6
17	*	40-49	6
18	*	10	6
19	*	11,12	6
20	90-93	**	6
21	90-93	H	6
22	94	**	6
23	94	H	6
24	*	40-49	2
25	*	10	2
26	*	11,12	2
27	90-93	**	2
28	94	**	2
29	*	28	2
30	95-96	**	4
31	*	40-49	0,1,3,7-9
32	*	10	0,1,3,7-9
33	*	11,12	0,1,3,7-9
34	90-93	**	0,1,3,7-9
35	94	**	0,1,3,7-9
36	*	28	0,1,3,7-9
37	95-96	**	0-3,5-9
38	90-94(95-96)	H	0-3,7-9(0-3,5-9)
39	97-99	**,H	0-3,5-9
40	97-99	**,H	4
41	95-96	H	4

* Denotes any visibility allowed, i.e., 90-99

** Denotes any present weather code except 10,11,12,28,40-49 or heavy present weather codes

H Denotes heavy present weather codes only: 30-39,59,62-65,67,69,72-75,81,82,84,86,88,90-99

TABLE III. Fog likelihood categories (FLC), groups (FLCG) and divisions (FLCGD) as used in study.

FLCG — (FLCGD)	Description	FLC
1 (I)	Heavy fog likely at observation time at station	1,2,4,6,7,11,17, 19,24,26,27,31,33
2 (II)	Light fog likely at observation time at station	3,5,9,13,18,25,32
3 (II)	Fog likely nearby, but not at observation time/station	15,16,29,36
4 (II)	Probably near fog in space and/ or time	8,10,30,40,41
5 (II)	Chance of fog at station and/or nearby station	20,22,28,34,35
6 (II)	Visibility qualifies for very light/light fog, but not reported	37
7 (III)	Fog very unlikely	12,14,21,23,38,39

TABLE IV(a). Statistical parameters for IR digital data, no cloud cover restrictions (see Appendices A and B for parameter information).

		All Reports	$\bar{T} \geq 269K$	$\bar{T} \geq 269K$ $S_{\bar{T}} < 2K$	$\bar{T} \geq 269K$ $S_{\bar{T}} \geq 2K$	$\bar{T} < 269K$	$\bar{T} < 269K$ $S_T \leq 2K$	$\bar{T} < 2$ $S_T >$
# cases	Div. I	168.	89.	61.	28.	79.	3.	76
	Div. II	60.	39.	28.	11.	21.	1.	4(
	Div. III	274.	146.	102.	44.	128.	9.	11
$\bar{T}$		267.84	279.06	280.78	275.34	255.22	262.07	254.
		265.87	277.28	276.67	276.88	255.01	267.95	254.6
		266.87	277.23	278.12	275.15	255.05	260.64	254.6
$\bar{T}_{STA}$		267.35	278.47	280.32	276.54	254.75	262.17	254.4
		265.51	277.27	278.91	275.09	254.33	269.00	253.
		267.04	277.4.	279.15	275.67	255.21	260.56	254.8
$\bar{S}_T$		4.08	1.31	0.77	4.09	0.64	1.48	0.8
		4.21	1.99	1.05	4.37	0.31	1.79	0.4
		3.74	1.91	0.96	4.27	0.33	1.35	0.1
$\overline{CV}_T$		0.02	0.01	0.00	0.01	0.03	0.01	0.0
		0.02	0.01	0.00	0.02	0.02	0.01	0.0
		0.01	0.01	0.00	0.02	0.02	0.01	0.0
$\overline{SK}_T$		-0.55	-0.53	-0.11	-1.41	-0.11	-0.16	-0.1
		-0.41	-0.68	-0.34	-1.45	-0.17	-0.72	-0.1
		-0.18	-0.32	0.02	-1.09	-0.33	0.58	-0.0
$\bar{G}_T$		1.85	0.80	0.41	1.87	0.83	0.79	3.1
		1.94	0.90	0.54	1.81	0.82	1.17	2.9
		1.81	0.89	0.49	1.83	2.87	0.97	3.0
$\bar{G}_{MIN_T}$		0.08	0.02	0.0	0.05	0.14	0.0	0.1
		0.08	0.02	0.0	0.05	0.13	0.0	0.1
		0.08	0.02	0.00	0.06	0.15	0.0	0.1
$\bar{G}_{MAX_T}$		5.86	3.01	1.48	6.34	7.08	2.29	9.34
		6.14	3.25	1.83	6.65	6.38	3.40	9.0
		5.28	3.07	1.80	6.47	7.30	2.75	8.1
$\bar{L}_T$		-0.02	-0.03	-0.03	-0.19	0.05	-0.01	0.05
		-0.01	-0.07	-0.05	-0.11	0.05	-0.03	0.0
		-0.00	-0.04	0.00	-0.13	0.04	0.00	0.04
$\bar{L}_{MIN_T}$		-12.19	-7.02	-5.17	-11.21	-17.27	-7.17	-17.06
		-12.54	-7.44	-6.55	-11.36	-16.94	-9.00	-17.14
		-11.75	-7.81	-6.16	-11.55	-16.13	-9.22	-16.71
$\bar{L}_{MAX_T}$		12.29	6.31	3.77	11.80	19.03	6.50	13.53
		11.86	6.77	4.18	12.59	16.71	9.50	15.89
		11.73	7.27	4.54	13.60	16.82	6.39	17.58

TABLE IV(b). Continued from IV(a).

		All Reports	$\bar{T} \geq 269K$	$\bar{T} \geq 269K$ $S_{\bar{T}} < 2K$	$\bar{T} > 269K$ $S_{\bar{T}} \geq 2K$	$\bar{T} < 269K$	$\bar{T} < 269K$ $S_T \leq 2K$	$\bar{T} < 269K$ $S_T > 2K$
# cases	Div. I	183.	107.	81.	26.	76.	3.	76.
	Div. II	80.	39.	25.	11.	41.	1.	40.
	Div. III	274.	146.	102.	44.	128.	9.	119.
$\bar{M}_T$		0.33	0.39	0.02	1.21	0.25	-0.07	0.27
		0.23	0.42	0.06	1.30	0.04	0.55	0.03
		0.35	0.38	0.07	1.15	0.32	-0.14	0.36
$\bar{R}_T$		10.12	7.99	5.52	17.71	23.23	6.33	25.03
		10.92	8.69	4.77	18.63	24.76	9.00	25.15
		14.89	8.27	4.65	16.09	22.45	8.56	23.66
$\overline{CFT}_{1\%}$		253.73	275.71	275.95	262.93	242.05	259.00	241.38
		250.07	271.75	275.91	261.18	242.33	263.00	241.81
		253.90	272.14	276.11	262.95	243.50	257.61	242.76
$\overline{CFT}_{16\%}$		263.77	277.46	280.13	271.71	248.33	260.50	247.85
		261.91	275.54	277.53	270.23	248.94	266.00	248.51
		263.03	275.52	277.31	271.38	248.77	259.39	247.97
$\overline{CFT}_{50\%}$		268.17	279.45	280.78	276.55	255.47	262.00	255.21
		266.39	277.71	279.70	275.15	255.05	266.50	254.71
		267.23	277.61	279.19	276.26	255.33	260.50	254.99
$\overline{CFT}_{84\%}$		271.35	280.59	281.56	276.71	262.03	263.67	262.01
		269.85	278.91	279.45	277.55	261.23	270.00	261.01
		270.03	278.36	278.36	278.31	261.23	261.78	261.19
$\overline{CFT}_{99\%}$		275.05	281.90	282.48	280.64	267.34	265.33	267.41
		273.60	280.49	280.06	279.66	267.09	272.00	266.96
		275.00	280.40	280.14	281.02	266.75	264.17	266.42
$\bar{P}_T^1$		0.34	0.34	0.35	0.32	0.35	0.25	0.35
		0.34	0.32	0.31	0.36	0.36	0.06	0.37
		0.36	0.34	0.35	0.35	0.37	0.37	0.37
$\bar{P}_T^2$		0.30	0.31	0.30	0.35	0.28	0.38	0.28
		0.28	0.28	0.27	0.26	0.29	0.31	0.28
		0.31	0.32	0.32	0.30	0.29	0.28	0.30
$\bar{P}_T^3$		0.35	0.34	0.34	0.33	0.37	0.38	0.36
		0.38	0.40	0.42	0.38	0.35	0.13	0.35
		0.34	0.34	0.33	0.36	0.33	0.40	0.33

TABLE IV(c). Statistical parameters for VIS digital data, no cloud cover restrictions.

		All Reports	$\bar{T} \geq 269K$	$\bar{T} \geq 269K$ $S_{\bar{T}} < 2K$	$\bar{T} > 269K$ $S_{\bar{T}} \geq 2K$	$\bar{T} < 269K$	$\bar{T} < 269K$ $S_T \leq 2K$	$\bar{T} < 26$ $S_T >$
# cases	Div. I	168.	89.	61.	28.	79.	3.	76
	Div. II	80.	39.	25.	11.	41.	1.	40
	Div. III	274.	146.	102.	44.	128.	9.	119
$\bar{A}$		131.75	117.63	116.29	120.53	147.67	155.36	147.3
		138.45	124.94	125.77	122.84	151.76	145.12	151.4
		129.76	113.63	114.68	111.37	148.14	156.79	147.4
$\bar{A}_{STA}$		131.75	116.97	115.90	119.71	148.37	156.67	148.0
		137.47	122.72	123.50	119.18	150.17	141.00	150.4
		130.37	114.67	115.10	111.63	148.27	157.33	147.5
$\bar{S}_A$		12.60	14.33	14.42	14.12	10.66	9.75	10.7
		13.35	16.37	15.49	16.61	10.48	8.59	10.5
		14.50	16.39	15.30	16.92	12.35	9.20	12.5
$\overline{CV}_A$		0.10	0.13	0.13	0.13	0.07	0.06	0.0
		0.11	0.14	0.12	0.17	0.08	0.06	0.0
		0.13	0.16	0.14	0.19	0.09	0.07	0.0
$\overline{SK}_A$		-0.21	-0.11	-0.12	-0.16	-0.32	-0.52	-0.3
		-0.30	-0.30	-0.34	-0.47	-0.25	-0.54	-0.2
		-0.22	-0.12	-0.12	-0.14	-0.32	-0.39	-0.3
$\bar{G}_A$		7.32	6.23	6.34	6.00	8.29	5.57	8.5
		8.05	9.00	9.07	10.36	6.33	5.66	8.3
		8.81	7.67	9.08	11.10	7.81	6.67	7.9
$\bar{G}_{MIN_A}$		0.68	0.78	0.78	0.89	0.57	0.24	0.5
		0.57	0.65	0.60	0.76	0.50	0.50	0.5
		0.72	0.80	0.81	0.78	0.62	0.67	0.6
$\bar{G}_{MAX_A}$		21.13	24.84	24.57	23.84	17.52	13.83	17.6
		23.16	29.08	28.68	30.22	17.53	16.28	17.5
		24.74	27.56	28.65	31.56	21.51	17.54	21.8
$\bar{L}_A$		-0.04	0.00	-0.06	0.32	-0.13	-0.44	-0.1
		-0.02	0.15	0.09	-0.27	-0.16	-1.02	-0.1
		-0.08	-0.08	0.02	-0.35	-0.03	-0.51	-0.0
$\bar{L}_{MIN_A}$		-59.27	-62.73	-60.21	-57.82	-46.67	-35.67	-47.3
		-61.74	-70.00	-70.57	-74.55	-46.17	-40.00	-48.3
		-71.03	-79.92	-72.50	-67.55	-60.98	-47.33	-61.9
$\bar{L}_{MAX_A}$		55.86	60.70	64.69	61.54	46.15	34.67	49.7
		60.00	81.03	80.45	74.91	52.33	55.00	52.8
		74.17	82.66	78.91	91.36	64.48	52.78	65.3

TABLE IV(d). Continued from IV(c).

		All Reports	$\bar{T} \geq 269K$	$\bar{T} \geq 269K$ $S_T < 2K$	$\bar{T} > 269K$ $S_T \geq 2K$	$\bar{T} < 269K$	$\bar{T} < 269K$ $S_T \leq 2K$	$\bar{T} < 269K$ $S_T > 2K$
# cases	Div. I	168.	89.	61.	28.	79.	3.	76.
	Div. II	80.	39.	23.	11.	41.	1.	40.
	Div. III	274.	146.	102.	44.	128.	9.	119.
$\bar{M}_A$		0.94	0.90	1.43	-0.25	0.97	1.31	0.96
		1.33	1.95	1.87	2.10	0.74	0.88	0.73
		1.24	1.38	1.43	1.29	1.03	0.32	1.14
$\bar{R}_A$		59.77	59.67	60.30	58.57	46.90	44.00	47.01
		67.02	69.13	69.68	77.91	45.51	34.00	46.80
		81.40	87.80	88.88	78.75	54.34	44.78	55.06
$\overline{CFA}_{1\%}$		104.13	87.81	88.75	94.29	122.51	130.00	122.21
		107.77	87.25	89.68	81.00	127.32	128.00	127.38
		98.01	79.45	81.54	74.61	119.18	132.89	118.14
$\overline{CFA}_{16\%}$		118.67	102.45	100.77	106.04	136.97	145.33	136.64
		124.67	107.69	109.66	102.64	140.83	136.00	140.95
		114.54	96.25	98.70	90.68	135.38	146.67	134.52
$\overline{CFA}_{50\%}$		132.69	116.53	117.72	120.29	148.65	156.67	148.33
		139.76	126.90	127.84	125.00	152.00	146.00	152.15
		131.02	115.07	116.11	112.66	149.22	157.11	148.62
$\overline{CFA}_{84\%}$		144.33	131.97	130.42	135.32	153.27	165.00	153.00
		151.52	140.77	140.86	140.55	151.76	165.00	151.97
		144.15	129.85	129.59	130.49	160.47	167.00	159.97
$\overline{CFA}_{99\%}$		157.89	147.67	145.72	151.66	169.41	174.00	169.22
		164.80	156.30	155.36	158.91	172.83	159.00	173.17
		157.41	147.05	145.20	151.34	175.52	177.67	175.20
$\bar{P}_A^1$		0.30	0.31	0.31	0.32	0.29	0.15	0.29
		0.27	0.31	0.31	0.29	0.24	0.31	0.24
		0.29	0.27	0.27	0.27	0.31	0.37	0.31
$\bar{P}_A^2$		0.29	0.28	0.27	0.26	0.30	0.22	0.31
		0.31	0.27	0.28	0.26	0.34	0.20	0.35
		0.31	0.31	0.31	0.32	0.30	0.25	0.31
$\bar{P}_A^3$		0.41	0.41	0.42	0.39	0.41	0.65	0.40
		0.42	0.42	0.41	0.43	0.41	0.49	0.41
		0.40	0.42	0.42	0.41	0.38	0.38	0.38

TABLE V(a). Statistical parameters for IR digital data, for $N \geq .8$.

		All Reports	$\bar{T} \geq 269K$	$\bar{T} > 269K$ $S_T < 2K$	$\bar{T} > 269K$ $S_T \geq 2K$	$\bar{T} < 269K$	$\bar{T} < 269K$ $S_T \leq 2K$	$\bar{T} < 26$ $S_T >$
# cases	Div. I	154.	82.	57.	25.	72.	3.	69
	Div. II	68.	29.	22.	7.	39.	1.	38
	Div. III	165.	66.	50.	16.	99.	8.	91
$\bar{\bar{T}}$		267.67	279.01	280.68	275.19	254.77	262.07	254.4
		263.69	276.68	277.86	272.98	254.38	267.95	254.0
		263.36	276.37	277.31	273.42	254.72	261.19	254.1
$\bar{T}_{STA}$		267.70	279.36	280.72	276.26	254.43	262.17	254.0
		263.60	276.43	276.25	270.71	254.06	269.00	253.6
		263.23	276.04	277.39	274.65	254.29	261.13	253.6
$\bar{S}_T$		4.03	1.75	0.77	3.92	6.66	1.48	5.8
		4.43	1.96	1.09	4.78	6.29	1.79	6.4
		4.03	1.67	0.85	4.21	5.69	1.40	6.0
$\overline{CV}_T$		0.02	0.01	0.00	0.01	0.03	0.01	0.0
		0.02	0.01	0.00	0.02	0.02	0.01	0.0
		0.02	0.01	0.00	0.02	0.02	0.01	0.0
$\overline{SK}_T$		-0.32	-0.52	-0.13	-1.42	-0.08	-0.16	-0.0
		-0.44	-0.73	-0.51	-1.67	-0.17	-0.72	-0.1
		-0.05	-0.13	0.17	-0.86	0.01	0.70	-0.0
$\bar{\bar{G}}_T$		1.86	0.77	0.41	1.57	3.11	0.79	3.2
		2.07	0.90	0.55	2.00	2.93	1.17	2.9
		2.01	0.78	0.46	1.77	2.83	0.91	2.9
$\bar{G}_{MIN_T}$		0.06	0.02	0.0	0.06	0.15	0.0	0.1
		0.08	0.02	0.0	0.09	0.13	0.0	0.1
		0.09	0.02	0.0	0.08	0.14	0.0	0.1
$\bar{G}_{MAX_T}$		5.64	2.98	1.30	6.29	9.11	2.79	9.4
		6.53	3.47	1.86	7.64	8.95	3.46	9.0
		5.70	2.71	1.30	6.18	7.69	2.82	8.1
$\bar{\bar{L}}_T$		-0.03	-0.09	-0.04	-0.21	0.04	-0.01	0.0
		-0.06	-0.06	-0.07	-0.04	0.04	-0.02	0.0
		0.04	0.00	0.01	-0.02	0.06	0.01	0.0
$\bar{L}_{MIN_T}$		-12.19	-7.59	-3.96	-11.26	-17.43	-7.17	-17.3
		-13.05	-7.75	-0.59	-11.50	-16.97	-9.00	-17.1
		-12.56	-7.40	-6.29	-11.00	-16.03	-9.31	-16.6
$\bar{L}_{MAX_T}$		12.05	6.07	3.78	13.30	13.95	8.50	19.3
		12.57	6.50	4.56	14.79	16.73	9.50	18.9
		12.32	7.13	4.09	14.75	16.52	8.94	17.4

TABLE V(b). Continued from V(a).

		All Reports	$\bar{T} \geq 269K$	$\bar{T} \geq 269K$ $S_T < 2K$	$\bar{T} \geq 269K$ $S_T \geq 2K$	$\bar{T} < 269K$	$\bar{T} < 269K$ $S_T \leq 2K$	$\bar{T} < 269K$ $S_T > 2K$
# cases	Div. I	154.	62.	37.	25.	72.	3.	69.
	Div. II	68.	29.	22.	7.	39.	1.	38.
	Div. III	165.	66.	50.	16.	99.	8.	91.
$\bar{M}_T$		0.20	0.35	0.03	1.09	0.21	-0.07	0.22
		0.19	0.40	0.10	1.38	0.03	0.55	0.02
		0.32	0.35	0.06	1.20	0.31	-0.12	0.35
$\bar{R}_T$		15.94	7.74	5.57	17.20	25.23	6.33	26.10
		17.93	8.69	4.89	20.29	24.87	8.00	25.29
		16.05	7.25	5.99	17.34	21.93	6.31	23.26
$\overline{CFT}_{1\%}$		250.92	274.05	275.04	269.14	241.65	257.00	240.93
		254.24	271.14	274.96	259.07	241.07	263.00	240.21
		259.16	272.03	273.31	261.78	245.94	257.94	242.71
$\overline{CFT}_{16\%}$		263.69	277.54	280.04	271.82	247.91	260.50	247.36
		259.71	274.91	275.86	266.79	246.40	266.00	247.93
		259.39	274.86	276.57	269.52	248.58	259.81	247.59
$\overline{CFT}_{50\%}$		267.96	279.36	280.71	276.26	254.97	262.00	254.67
		264.08	277.09	277.95	274.36	254.41	268.50	254.04
		268.70	276.70	277.37	274.63	255.03	261.06	254.50
$\overline{CFT}_{84\%}$		271.66	280.43	281.29	276.96	261.67	263.67	261.59
		268.39	278.26	278.68	276.91	260.53	270.00	260.28
		267.53	277.85	278.36	277.03	260.87	262.38	260.52
$\overline{CFT}_{99\%}$		274.86	281.80	282.41	280.46	266.96	265.33	267.03
		272.17	279.74	279.86	279.30	266.54	272.00	266.39
		271.22	279.25	279.80	279.15	265.97	264.75	265.97
$\bar{P}_T^1$		0.34	0.34	0.34	0.33	0.34	0.25	0.35
		0.35	0.33	0.31	0.40	0.36	0.06	0.37
		0.36	0.33	0.35	0.32	0.37	0.27	0.38
$\bar{P}_T^2$		0.30	0.31	0.30	0.34	0.23	0.38	0.23
		0.29	0.29	0.28	0.33	0.29	0.81	0.25
		0.30	0.31	0.33	0.27	0.29	0.21	0.30
$\bar{P}_T^3$		0.35	0.34	0.34	0.33	0.37	0.38	0.37
		0.36	0.33	0.41	0.26	0.34	0.13	0.35
		0.34	0.35	0.34	0.41	0.34	0.42	0.33

TABLE V(c). Statistical parameters for VIS data, $N \geq .8$.

# cases	All Reports	$\bar{T} \geq 269K$	$\bar{T} > 269K$ $S_{\bar{T}} < 2K$	$\bar{T} > 269K$ $S_{\bar{T}} \geq 2K$	$\bar{T} < 269K$	$\bar{T} < 269K$ $S_T \leq 2K$	$\bar{T} < 26$ $S_T >$
Div. I	454.	82.	57.	25.	72.	3.	69.
Div. II	68.	29.	22.	7.	39.	1.	38.
Div. III	165.	66.	50.	16.	99.	8.	91.
$\bar{A}$	132.77	119.59	117.56	124.22	147.78	155.36	147.45
	145.52	134.40	134.19	135.05	153.79	145.12	154.02
	144.30	131.52	131.06	132.15	152.95	157.58	152.54
$\bar{A}_{STA}$	133.08	119.25	119.26	119.26	146.79	156.67	148.45
	145.28	136.06	136.45	134.57	152.18	141.00	152.47
	145.36	134.71	135.54	132.15	152.45	157.38	152.09
$\bar{S}_A$	12.61	14.55	14.69	13.55	10.53	9.79	10.66
	11.97	14.93	15.14	14.20	9.77	8.59	9.80
	12.67	15.36	15.27	15.64	10.67	9.67	10.95
$\overline{CV}_A$	0.10	0.15	0.15	0.12	0.07	0.06	0.07
	0.09	0.12	0.12	0.11	0.07	0.06	0.07
	0.10	0.13	0.12	0.13	0.08	0.07	0.08
$\overline{SK}_A$	-0.25	-0.13	-0.14	-0.16	-0.31	-0.53	-0.30
	-0.39	-0.58	-0.57	-0.63	-0.24	-0.54	-0.23
	-0.37	-0.47	-0.50	-0.46	-0.32	-0.37	-0.32
$\bar{G}_A$	7.34	8.26	8.46	7.81	6.29	5.57	6.32
	7.56	9.11	9.54	7.75	6.05	5.66	6.06
	7.65	9.09	8.76	10.31	6.98	6.81	7.00
$\bar{G}_{MIN_A}$	0.69	0.79	0.72	0.95	0.57	0.24	0.58
	0.55	0.60	0.66	0.51	0.50	0.50	0.50
	0.58	0.85	0.77	1.01	0.58	0.75	0.56
$\bar{G}_{MAX_A}$	21.05	24.05	24.69	22.54	17.60	13.83	17.76
	21.21	27.09	28.35	23.13	16.35	16.28	16.86
	21.78	25.44	25.03	26.71	19.34	18.22	19.44
$\bar{L}_A$	-0.06	-0.02	-0.10	0.14	-0.10	-0.44	-0.03
	-0.09	-0.09	0.25	-0.17	-0.03	-0.07	-0.05
	-0.16	-0.13	0.07	-0.98	-0.05	-0.34	-0.02
$\bar{L}_{MIN_A}$	-54.20	-61.09	-64.37	-53.65	-46.36	-35.67	-46.83
	-54.76	-64.79	-66.66	-52.00	-47.31	-43.00	-47.59
	-62.67	-74.08	-68.14	-92.31	-55.07	-49.13	-55.59
$\bar{L}_{MAX_A}$	58.49	62.67	64.76	58.04	49.44	34.67	50.09
	60.79	74.62	79.73	56.57	50.51	55.00	50.39
	63.62	80.00	77.46	98.15	60.04	53.00	60.66

TABLE V(d). Continued from V(c).

	All Reports	$\bar{T} \geq 269K$	$\bar{T} > 269K$ $S_T < 2K$	$\bar{T} > 269K$ $S_T \geq 2K$	$\bar{T} < 269K$	$\bar{T} < 269K$ $S_T \leq 2K$	$\bar{T} < 269K$ $S_T > 2K$
# cases Div. I	154.	82.	57.	25.	72.	3.	69.
Div. II	68.	29.	22.	7.	39.	1.	38.
Div. III	165.	66.	50.	16.	99.	8.	91.
$\bar{M}_A$	1.09	1.10	1.40	0.50	1.00	1.31	0.98
	1.36	2.53	2.50	2.38	0.49	0.88	0.48
	1.29	2.01	2.22	1.38	0.81	0.30	0.86
$\bar{R}_A$	55.08	59.95	60.65	58.36	46.53	44.00	46.64
	52.31	65.38	64.59	61.57	43.72	34.00	43.97
	55.39	64.21	63.36	66.81	49.52	45.13	49.90
$\overline{CFA}_{1\%}$	104.96	99.53	98.66	95.50	122.76	130.00	122.45
	110.56	97.14	96.77	96.29	131.00	125.00	131.16
	114.03	95.53	95.16	96.63	126.36	133.63	125.73
$\overline{CFA}_{16\%}$	119.65	104.27	101.74	110.04	137.17	145.33	136.81
	133.28	118.45	118.14	119.57	144.23	136.00	144.50
	131.56	119.14	119.14	119.13	142.13	147.13	141.75
$\overline{CFA}_{50\%}$	133.86	126.76	119.04	124.72	146.78	156.67	146.43
	145.88	136.93	136.77	137.43	154.25	146.00	154.50
	143.59	135.33	133.24	133.50	153.76	157.88	153.40
$\overline{CFA}_{84\%}$	143.29	135.85	132.07	137.92	153.32	165.00	152.03
	157.24	146.79	145.56	146.57	165.51	158.00	165.79
	156.65	146.47	146.00	147.94	163.78	167.88	163.42
$\overline{CFA}_{99\%}$	154.84	149.28	147.25	153.92	169.29	174.00	169.09
	166.87	161.06	161.36	159.86	174.72	159.00	175.13
	169.42	159.74	158.56	162.44	175.83	178.75	175.63
$\bar{P}_A^1$	0.31	0.32	0.31	0.34	0.29	0.15	0.30
	0.25	0.27	0.27	0.27	0.24	0.31	0.24
	0.30	0.26	0.27	0.25	0.32	0.38	0.31
$\bar{P}_A^2$	0.29	0.28	0.27	0.29	0.30	0.22	0.30
	0.32	0.28	0.28	0.28	0.35	0.20	0.35
	0.31	0.31	0.31	0.33	0.30	0.26	0.31
$\bar{P}_A^3$	0.41	0.40	0.41	0.38	0.41	0.63	0.40
	0.43	0.43	0.42	0.45	0.41	0.49	0.41
	0.40	0.42	0.42	0.42	0.38	0.38	0.38

TABLE VI(a). Statistical parameters for N and $N_h \geq .8$.

		All Reports	$\bar{T} \geq 269K$	$\bar{T} \geq 269K$ $S_T < 2K$	$\bar{T} \geq 269K$ $S_T \geq 2K$	$\bar{T} < 269K$	$\bar{T} < 269K$ $S_T \leq 2K$	$\bar{T} < 2$ $S_T >$
# cases	Div. I	152.	80.	55.	25.	72.	3.	69
	Div. II	63.	27.	20.	7.	36.	1.	35
	Div. III	145.	58.	46.	12.	87.	8.	79
$\bar{\bar{T}}$		267.51	278.97	280.69	275.19	254.77	262.07	254.4
		264.27	276.15	277.26	272.98	255.35	267.95	254.9
		263.46	276.47	277.42	272.84	254.73	261.19	254.1
$\bar{\bar{T}}_{STA}$		267.55	279.39	280.75	276.26	254.43	262.17	254.0
		264.06	275.87	277.07	270.71	255.19	269.60	254.8
		263.36	276.77	277.46	274.35	254.42	261.13	253.7
$\bar{S}_T$		4.07	1.75	0.76	3.92	0.66	1.48	6.8
		4.46	2.08	1.14	5.76	0.15	1.79	6.2
		4.07	1.53	0.85	4.14	0.77	1.46	6.2
$\overline{CV}_T$		0.02	0.01	0.00	0.01	0.03	0.01	0.0
		0.02	0.01	0.00	0.02	0.02	0.01	0.0
		0.02	0.01	0.00	0.02	0.02	0.01	0.0
$\overline{SK}_T$		-0.29	-0.48	-0.06	-1.42	-0.03	-0.16	-0.0
		-0.49	-0.80	-0.56	-1.67	-0.26	-0.72	-0.3
		-0.07	-0.14	0.10	-1.05	-0.02	0.20	-0.0
$\bar{\bar{G}}_T$		1.86	0.77	0.41	1.57	3.11	0.79	3.2
		2.07	0.95	0.58	2.06	2.92	1.17	2.9
		2.00	0.76	0.46	1.87	2.83	0.91	3.0
$\bar{G}_{MIN_T}$		0.08	0.02	0.0	0.06	0.15	0.0	0.1
		0.09	0.02	0.0	0.09	0.14	0.0	0.1
		0.09	0.02	0.0	0.09	0.14	0.0	0.1
$\bar{G}_{MAX_T}$		5.88	2.98	1.48	6.29	9.11	2.29	9.4
		6.53	3.45	1.56	7.64	8.84	3.40	8.9
		5.72	2.65	1.59	6.71	7.76	2.92	8.2
$\bar{\bar{L}}_T$		-0.03	-0.09	-0.03	-0.21	0.04	-0.01	0.0
		-0.04	-0.07	-0.08	-0.04	-0.01	-0.02	-0.0
		0.01	-0.00	0.01	-0.06	0.01	0.01	0.0
$\bar{L}_{MIN_T}$		-12.29	-7.51	-5.52	-11.26	-17.43	-7.17	-17.8
		-13.22	-8.02	-6.80	-11.50	-17.13	-9.00	-17.3
		-12.65	-7.55	-6.50	-12.21	-16.06	-9.31	-16.7
$\bar{L}_{MAX_T}$		12.10	6.14	3.80	11.30	18.85	6.50	19.3
		12.33	6.72	4.00	12.79	18.54	9.50	18.7
		12.63	7.02	4.02	16.21	18.70	6.94	17.6

TABLE VI(b). Continued from VI(a).

		All Reports	$\bar{T} \geq 269K$	$\bar{T} > 269K$ $S_T < 2K$	$\bar{T} > 269K$ $S_T \geq 2K$	$\bar{T} < 269K$	$\bar{T} < 269K$ $S_T \leq 2K$	$\bar{T} < 269K$ $S_T > 2K$
# cases	Div. I	152.	80.	55.	25.	72.	3.	69.
	Div. II	63.	27.	20.	7.	36.	1.	35.
	Div. III	145.	58.	46.	12.	87.	8.	79.
$\bar{M}_T$		0.29	0.36	0.03	1.09	0.21	-0.07	0.22
		0.21	0.44	0.11	1.38	0.04	0.55	0.02
		0.36	0.38	0.37	1.26	0.39	-0.13	0.44
$\bar{R}_T$		16.07	7.79	3.46	17.26	25.28	8.33	26.10
		17.72	9.07	5.15	20.29	24.21	9.00	24.54
		15.96	8.89	4.01	17.50	22.06	8.81	23.61
$\overline{CFT}_{1\%}$		258.68	275.99	278.92	255.14	241.83	259.00	240.93
		264.45	276.50	274.22	259.07	242.53	263.00	241.94
		255.22	272.37	275.40	250.75	243.79	257.94	242.36
$\overline{CFT}_{16\%}$		263.48	277.49	280.06	271.82	247.91	260.50	247.36
		260.15	274.31	276.25	268.75	249.50	266.00	249.03
		259.17	275.14	276.67	269.25	246.52	259.81	247.37
$\overline{CFT}_{50\%}$		267.79	279.33	280.72	276.28	254.97	262.00	254.67
		264.48	276.59	277.38	274.50	255.39	263.50	255.01
		263.81	276.76	277.49	274.04	255.17	261.06	254.57
$\overline{CFT}_{84\%}$		271.55	280.41	281.29	278.48	261.67	265.67	261.59
		268.44	277.80	278.16	276.93	261.43	270.00	261.19
		267.59	277.79	278.18	276.29	260.79	262.38	260.63
$\overline{CFT}_{99\%}$		274.76	281.77	282.46	280.40	266.90	269.33	267.03
		272.15	279.37	279.36	279.30	266.74	272.00	266.59
		271.13	279.17	279.41	278.29	265.86	264.75	265.97
$\bar{P}_T^1$		0.34	0.34	0.35	0.33	0.34	0.25	0.35
		0.34	0.34	0.32	0.40	0.34	0.06	0.35
		0.35	0.35	0.32	0.34	0.37	0.37	0.37
$\bar{P}_T^2$		0.30	0.32	0.31	0.34	0.29	0.38	0.28
		0.30	0.30	0.29	0.33	0.30	0.31	0.29
		0.30	0.31	0.35	0.22	0.29	0.21	0.30
$\bar{P}_T^3$		0.35	0.35	0.33	0.35	0.37	0.38	0.37
		0.35	0.35	0.39	0.26	0.35	0.13	0.36
		0.35	0.37	0.35	0.44	0.34	0.42	0.33

TABLE VI(c). Statistical parameters for VIS data N and $N_h \geq .8$.

		All Reports	$\bar{T} \geq 269K$	$\bar{T} > 269K$ $S_T < 2K$	$\bar{T} > 269K$ $S_T \geq 2K$	$\bar{T} < 269K$	$\bar{T} < 269K$ $S_T \leq 2K$	$\bar{T} < 2$ $S_T >$
# cases	Div. I	152.	80.	55.	25.	72.	8.	6
	Div. II	63.	27.	20.	7.	36.	1.	3
	Div. III	145.	58.	46.	12.	87.	8.	7
$\bar{A}$		133.33	120.31	118.54	124.22	147.78	155.36	147.
		145.30	135.94	136.25	135.05	152.32	145.12	152.
		144.81	132.14	131.10	136.17	153.26	157.58	152.
$\bar{A}_{STA}$		133.82	120.35	120.04	117.28	148.79	156.67	148.
		143.95	135.50	135.55	134.57	150.44	141.00	150.
		143.89	135.25	135.46	134.36	152.97	157.38	152.
$\bar{S}_A$		12.52	14.28	14.54	13.58	10.63	9.78	10.
		11.72	13.99	13.86	14.30	10.02	8.59	10.
		12.45	14.39	13.09	14.61	10.73	9.97	10.
$\overline{CV}_A$		0.10	0.13	0.13	0.12	0.07	0.06	0.
		0.09	0.11	0.11	0.11	0.07	0.06	0.
		0.09	0.12	0.12	0.12	0.07	0.07	0.
$\overline{SK}_A$		-0.23	-0.15	-0.15	-0.16	-0.31	-0.53	-0.
		-0.37	-0.38	-0.57	-0.65	-0.20	-0.34	-0.
		-0.37	-0.50	-0.47	-0.61	-0.28	-0.27	-0.
$\bar{G}_A$		7.76	8.17	8.32	7.61	8.29	9.57	8.
		7.23	8.62	8.45	7.75	8.19	8.66	8.
		7.82	8.71	8.42	8.81	8.90	8.81	8.
$\bar{G}_{MIN_A}$		0.66	0.78	0.70	0.99	0.57	0.24	0.
		0.55	0.57	0.55	0.61	0.50	0.50	0.
		0.69	0.84	0.76	1.15	0.59	0.75	0.
$\bar{G}_{MAX_A}$		20.69	23.35	24.45	22.54	17.60	13.83	17.
		20.87	25.62	25.49	23.15	17.30	16.28	17.
		21.22	24.54	24.27	25.57	19.01	18.22	19.
$\bar{L}_A$		-0.05	-0.01	-0.08	0.14	-0.10	-0.44	-0.
		-0.07	-0.14	0.22	-1.17	-0.02	-1.02	0.
		-0.06	-0.21	-0.04	-0.87	0.05	-0.39	0.
$\bar{L}_{MIN_A}$		-53.74	-60.38	-63.45	-53.60	-46.36	-35.67	-46.
		-54.49	-62.07	-66.40	-52.00	-46.36	-40.00	-48.
		-60.24	-66.34	-64.76	-62.08	-54.84	-49.13	-55.
$\bar{L}_{MAX_A}$		56.43	62.71	64.84	58.04	49.44	34.67	50.
		60.67	72.37	77.40	56.57	51.89	55.00	51.
		64.95	74.80	72.17	65.92	58.48	53.00	59.

TABLE VI(d). Continued from VI(c).

	All Reports	$\bar{T} \geq 269K$	$\bar{T} \geq 269K$ $S_{\bar{T}} < 2K$	$\bar{T} \geq 269K$ $S_{\bar{T}} \geq 2K$	$\bar{T} < 269K$	$\bar{T} < 269K$ $S_T \leq 2K$	$\bar{T} < 269K$ $S_T > 2K$
# cases Div. I	152.	80.	55.	25.	72.	3.	69.
Div. II	63.	27.	20.	7.	36.	1.	35.
Div. III	145.	58.	46.	12.	87.	8.	79.
$\bar{M}_A$	1.08	1.10	1.46	0.50	1.00	1.31	0.98
	1.13	1.98	1.65	2.38	0.48	0.88	0.47
	1.20	1.99	2.10	1.58	0.63	0.20	0.71
$\bar{R}_A$	53.53	59.84	60.51	58.36	46.53	44.00	46.64
	51.86	61.59	61.80	61.57	44.50	34.00	44.86
	54.53	62.55	62.24	63.75	48.85	45.13	49.23
$\overline{CFA}_{1\%}$	103.51	99.99	97.45	99.56	122.76	130.00	122.45
	110.70	100.07	100.70	98.29	129.17	125.00	129.29
	115.32	97.14	96.22	100.67	127.44	133.63	126.81
$\overline{CFA}_{16\%}$	120.33	105.17	102.96	110.04	137.17	145.33	136.81
	133.51	121.52	121.20	119.57	142.50	136.00	142.69
	132.03	116.26	115.09	120.75	142.54	147.13	142.08
$\overline{CFA}_{50\%}$	134.41	121.47	120.00	124.72	143.73	156.67	143.43
	140.43	137.93	138.10	137.43	142.81	146.00	143.00
	140.01	134.14	131.20	137.75	143.93	157.88	143.53
$\overline{CFA}_{84\%}$	142.74	134.42	132.64	137.92	148.32	155.00	148.03
	150.81	149.46	149.80	146.57	152.31	153.00	152.57
	157.15	146.90	145.93	150.58	163.90	167.32	163.59
$\overline{CFA}_{99\%}$	159.05	149.82	147.96	155.92	169.29	174.00	169.09
	168.56	161.67	162.36	159.86	173.72	159.00	174.14
	169.65	159.69	158.46	164.42	176.29	173.75	176.64
$\bar{P}_A^1$	0.31	0.32	0.32	0.34	0.29	0.15	0.30
	0.26	0.23	0.26	0.27	0.25	0.31	0.25
	0.30	0.27	0.27	0.26	0.32	0.38	0.31
$\bar{P}_A^2$	0.29	0.26	0.27	0.25	0.30	0.22	0.30
	0.31	0.27	0.27	0.28	0.35	0.20	0.35
	0.30	0.30	0.31	0.29	0.30	0.26	0.30
$\bar{P}_A^3$	0.41	0.40	0.41	0.36	0.41	0.63	0.40
	0.43	0.45	0.43	0.45	0.40	0.49	0.40
	0.40	0.43	0.43	0.44	0.38	0.36	0.38

TABLE VII(a). Statistical parameters for IR digital data, for N and $N_h \geq .8$, south-component wind directions (100° to 270°).

		All Reports	$\bar{T} \geq 269K$	$\bar{T} \geq 269K$ $S_T < 2K$	$\bar{T} > 269K$ $S_T \geq 2K$	$\bar{T} < 269K$	$\bar{T} < 269K$ $S_T \leq 2K$	$\bar{T} <$ S_T
# cases	Div. I	114.	58.	43.	15.	53.	2.	5
	Div. II	47.	18.	14.	4.	29.	0.	4
	Div. III	87.	22.	17.	5.	65.	6.	5
$\bar{\bar{T}}$		260.25	270.99	269.17	275.59	252.23	259.71	251.
		263.74	270.70	271.76	272.93	255.70	0.0	255.
		258.66	270.16	270.39	273.39	252.76	261.63	251.
$\bar{T}_{STA}$		260.17	270.29	269.20	276.76	251.80	259.75	251.
		263.69	270.73	270.94	271.25	255.59	0.0	255.
		258.39	270.20	270.79	274.20	252.35	261.42	251.
$\bar{S}_T$		4.39	1.53	0.76	5.73	0.93	1.40	7.
		4.72	2.10	1.24	5.15	0.54	0.0	6.
		4.80	1.52	0.97	5.40	5.64	1.57	5.
$\bar{CV}_T$		0.02	0.01	0.00	0.01	0.03	0.01	0.
		0.02	0.01	0.00	0.02	0.02	0.0	0.
		0.02	0.01	0.00	0.01	0.02	0.01	0.
$\bar{SK}_T$		-0.24	-0.43	-0.04	-1.54	-0.04	-0.08	-0.
		-0.44	-0.56	-0.00	-0.76	-0.37	0.0	-0.
		-0.07	-0.34	-0.15	-1.08	0.02	-0.00	0.
$\bar{G}_T$		1.72	0.70	0.41	1.51	3.26	0.80	3.
		2.25	0.99	0.84	2.20	3.04	0.0	3.
		2.30	0.77	0.51	1.65	2.92	1.04	3.
$\bar{G}_{MIN_T}$		0.09	0.01	0.0	0.05	0.18	0.0	0.
		0.05	0.02	0.0	0.03	0.13	0.0	0.
		0.10	0.02	0.0	0.07	0.13	0.0	0.
$\bar{G}_{MAX_T}$		5.91	2.03	1.47	9.95	9.49	2.57	7.
		5.70	3.13	2.16	8.78	8.89	0.0	8.
		6.42	2.75	1.75	8.14	7.66	3.73	8.
$\bar{L}_T$		-0.04	-0.05	-0.05	-0.28	0.02	-0.12	0.
		-0.05	-0.05	-0.04	0.04	-0.04	0.0	-0.
		-0.01	-0.01	-0.01	-0.05	-0.01	0.00	-0.
$\bar{L}_{MIN_T}$		-12.40	-7.25	-5.97	-11.05	-16.01	-7.75	-18.
		-13.50	-8.38	-7.16	-11.25	-16.97	0.0	-16.
		-14.24	-7.73	-5.50	-11.90	-16.44	-9.33	-17.
$\bar{L}_{MAX_T}$		12.05	5.56	3.74	14.17	16.00	7.50	19.
		13.35	7.44	5.14	15.50	17.02	0.0	17.
		14.06	7.36	5.55	13.40	16.33	7.58	17.

TABLE VII(b). Continued from VII(a).

	All Reports	$\bar{T} \geq 269K$	$\bar{T} > 269K$ $S_{\bar{T}} < 2K$	$\bar{T} > 269K$ $S_{\bar{T}} \geq 2K$	$\bar{T} < 269K$	$\bar{T} < 269K$ $S_T \leq 2K$	$\bar{T} < 269K$ $S_T > 2K$
# cases Div. I	111.	58.	43.	15.	53.	2.	51.
Div. II	47.	18.	14.	4.	29.	0.	29.
Div. III	87.	22.	17.	5.	65.	6.	59.
$\bar{M}_T$	0.10	0.32	0.03	1.14	-0.02	-0.21	-0.01
	0.30	0.41	0.15	1.32	0.23	0.0	0.23
	0.13	0.17	0.09	0.61	0.11	-0.13	0.14
$\bar{R}_T$	16.05	8.87	5.47	19.65	20.05	6.00	26.83
	18.40	8.47	5.30	19.33	24.69	0.0	24.66
	18.06	8.86	4.71	15.50	21.92	7.50	23.38
$\overline{CFT}_{1\%}$	267.84	274.56	276.41	269.60	259.11	257.00	238.41
	253.32	271.89	274.64	261.20	241.97	0.0	241.97
	249.75	272.16	274.29	264.90	242.16	258.00	240.55
$\overline{CFT}_{16\%}$	282.16	277.89	279.55	272.46	249.21	256.25	244.70
	259.11	274.61	276.61	267.63	249.43	0.0	249.43
	253.94	274.82	276.09	270.50	246.37	260.00	245.53
$\overline{CFT}_{50\%}$	266.39	279.30	280.20	276.73	252.25	259.50	251.97
	264.04	277.11	277.93	274.25	255.93	0.0	255.93
	258.79	276.27	276.94	274.00	252.67	261.50	251.99
$\overline{CFT}_{84\%}$	270.30	280.20	280.77	276.57	259.69	261.25	259.54
	268.52	278.53	278.75	277.75	262.31	0.0	262.31
	263.44	277.43	277.56	276.00	258.71	263.00	258.27
$\overline{CFT}_{99\%}$	275.67	281.42	281.67	280.23	265.15	263.00	265.24
	271.81	280.17	280.06	280.75	266.62	0.0	266.62
	267.80	279.82	279.66	279.20	264.03	265.50	263.93
$\bar{P}_T^1$	0.33	0.33	0.34	0.31	0.34	0.21	0.34
	0.34	0.33	0.31	0.31	0.34	0.0	0.34
	0.36	0.31	0.31	0.26	0.33	0.40	0.33
$\bar{P}_T^2$	0.30	0.30	0.29	0.34	0.29	0.46	0.28
	0.31	0.35	0.33	0.37	0.29	0.3	0.29
	0.29	0.29	0.32	0.16	0.29	0.22	0.30
$\bar{P}_T^3$	0.36	0.35	0.35	0.35	0.37	0.32	0.39
	0.35	0.32	0.34	0.24	0.37	0.0	0.37
	0.35	0.41	0.35	0.59	0.33	0.38	0.33

TABLE VII(c). Statistical parameters for VIS digital data for N and $N_h \geq .8$, south-component wind directions (100° to 270°).

		All Reports	$\bar{T} \geq 269K$	$\bar{T} \geq 269K$ $S_T < 2K$	$\bar{T} \geq 269K$ $S_T \geq 2K$	$\bar{T} < 269K$	$\bar{T} < 269K$ $S_T \leq 2K$	$\bar{T} < 2$ $S_T >$
# cases	Div. I	111.	58.	43.	15.	53.	2.	51
	Div. II	47.	18.	14.	4.	29.	0.	29
	Div. III	87.	22.	17.	5.	65.	6.	59
$\bar{A}$		139.25	122.53	118.96	132.77	149.17	164.18	148.5
		144.74	138.36	139.00	141.11	143.94	0.0	149.9
		151.60	136.45	135.34	149.30	156.80	163.29	156.1
$\bar{A}_{STA}$		139.69	122.72	121.91	129.07	149.87	167.50	149.1
		143.11	134.44	139.14	139.00	146.43	0.0	148.4
		155.15	140.55	139.24	145.00	157.33	165.93	156.5
$\bar{S}_A$		12.0.	10.74	9.35	11.9e	10.11	8.57	10.1
		11.25	12.93	10.32	11.51	10.20	0.0	10.2
		10.94	15.15	10.16	11.63	9.52	0.94	9.5
$\overline{CV}_A$		0.10	0.12	0.13	0.10	0.07	0.05	0.0
		0.08	0.10	0.10	0.08	0.07	0.0	0.0
		0.08	0.12	0.13	0.08	0.06	0.06	0.0
$\overline{SK}_A$		-0.24	-0.10	-0.15	-0.20	-0.33	-0.66	-0.3
		-0.35	-0.01	-0.07	-0.77	-0.19	0.0	-0.1
		-0.38	-0.03	-0.06	-0.49	-0.27	-0.31	-0.2
$\bar{G}_A$		7.12	8.14	8.27	7.64	6.99	4.96	6.0
		7.00	8.05	8.21	7.59	6.86	0.0	6.3
		7.00	8.90	9.07	6.39	6.33	5.68	6.3
$\bar{G}_{MIN_A}$		0.66	0.70	0.71	0.59	0.52	0.0	0.5
		0.54	0.58	0.52	0.78	0.52	0.0	0.5
		0.66	0.67	0.76	1.22	0.59	0.69	0.5
$\bar{G}_{MAX_A}$		20.62	24.05	24.57	21.69	18.00	13.14	17.9
		19.78	25.51	24.55	20.59	17.47	0.0	17.4
		19.50	26.11	27.50	21.37	17.25	18.63	17.1
$\bar{L}_A$		0.03	0.11	-0.00	0.45	-0.05	0.30	-0.0
		-0.25	-0.63	-0.43	-1.31	-0.01	0.0	-0.0
		0.20	0.39	0.41	0.31	0.14	-0.80	0.2
$\bar{L}_{MIN_A}$		-53.26	-51.14	-54.42	-51.75	-44.64	-38.00	-44.9
		-53.02	-59.07	-61.71	-52.50	-46.90	0.0	-43.8
		-53.97	-55.25	-63.94	-59.00	-50.15	-53.17	-47.8
$\bar{L}_{MAX_A}$		56.56	65.00	65.85	62.47	47.21	33.50	47.7
		59.02	71.57	75.57	56.75	51.34	0.0	51.3
		59.47	75.64	77.32	68.20	54.00	55.67	52.8

TABLE VII(d). Continued from VII(c).

	All Reports	$\bar{T} \geq 269K$	$\bar{T} \geq 269K$ $S_T < 2K$	$\bar{T} \geq 269K$ $S_T \geq 2K$	$\bar{T} < 269K$	$\bar{T} < 269K$ $S_T \leq 2K$	$\bar{T} < 269K$ $S_T > 2K$
# cases Div. I	141.	58.	43.	15.	53.	2.	51.
Div. II	47.	13.	4.	4.	29.	0.	29.
Div. III	87.	22.	17.	5.	65.	6.	59.
$\bar{M}_A$	1.11	1.26	1.36	1.03	0.92	0.92	0.92
	1.03	2.03	2.07	1.89	0.40	0.0	0.40
	1.17	2.73	2.95	1.90	0.64	0.21	0.69
$\bar{R}_A$	51.94	58.95	60.67	54.80	44.23	41.00	44.41
	50.43	58.22	59.14	56.00	45.59	0.0	45.59
	49.29	64.55	67.18	58.60	44.12	40.67	44.47
$\overline{CFA}_{1\%}$	103.06	92.17	87.72	104.93	125.45	139.50	124.90
	117.28	102.28	100.79	107.50	126.59	0.0	126.59
	124.97	98.95	94.29	114.60	133.77	140.33	133.05
$\overline{CFA}_{16\%}$	122.76	107.90	103.50	120.33	139.02	150.00	138.35
	133.04	125.33	121.43	136.00	140.03	0.0	140.03
	140.44	120.36	116.47	133.60	147.33	155.83	146.50
$\overline{CFA}_{50\%}$	136.30	123.84	120.23	132.80	150.09	165.00	149.51
	145.77	136.39	137.07	143.00	150.34	0.0	150.34
	152.63	136.10	130.62	147.20	157.45	163.50	156.83
$\overline{CFA}_{84\%}$	147.07	135.97	133.02	144.40	159.23	172.50	155.71
	155.91	149.06	148.36	151.50	160.17	0.0	160.17
	162.20	150.91	149.24	156.60	166.11	172.67	165.44
$\overline{CFA}_{99\%}$	160.06	151.10	148.09	155.73	169.74	180.50	169.31
	167.70	160.50	159.93	162.50	172.17	0.0	172.17
	174.25	165.50	161.47	170.40	177.19	181.50	177.53
$\bar{P}_A^1$	0.29	0.29	0.29	0.34	0.23	0.20	0.23
	0.25	0.25	0.27	0.33	0.24	0.0	0.24
	0.31	0.27	0.26	0.30	0.32	0.33	0.31
$\bar{P}_A^2$	0.29	0.26	0.29	0.27	0.31	0.27	0.31
	0.31	0.29	0.28	0.32	0.33	0.0	0.33
	0.31	0.32	0.32	0.32	0.31	0.30	0.31
$\bar{P}_A^3$	0.42	0.42	0.43	0.42	0.41	0.53	0.41
	0.44	0.43	0.45	0.38	0.44	0.0	0.44
	0.38	0.41	0.42	0.38	0.37	0.32	0.37

TABLE VIII(a). Statistical parameters for IR digital data for N and $N_h \geq .8$, north-component winds (280° to 090°).

	All Reports	$\bar{T} \geq 269K$	$\bar{T} \geq 269K$ $S_T < 2K$	$\bar{T} \geq 269K$ $S_T \geq 2K$	$\bar{T} < 269K$	$\bar{T} < 269K$ $S_T \leq 2K$	$\bar{T} <$ $S_T >$
# cases Div. I							
Div. II	38.	20.	12.	8.	18.	1.	
Div. III	16.	9.	6.	3.	7.	1.	
	55.	36.	29.	7.	19.	2.	
$\bar{\bar{T}}$	270.75	278.96	282.57	273.61	261.60	266.78	261.
	265.80	275.05	276.06	275.05	253.91	267.95	251.
	271.35	276.71	277.73	274.45	261.15	259.86	261.
$\bar{T}_{STA}$	271.00	279.40	282.75	274.38	261.67	267.00	261.
	265.13	274.11	276.17	270.00	253.57	269.00	251.
	271.00	277.11	277.76	274.45	261.15	260.25	261.
$\bar{S}_T$	4.09	2.24	0.78	4.45	0.14	1.42	6.
	5.48	2.04	0.91	4.21	5.33	1.75	5.
	3.07	1.55	0.77	4.68	0.04	0.91	0.
$\overline{CV}_T$	0.02	0.01	0.00	0.02	0.02	0.01	0.
	0.01	0.01	0.00	0.02	0.02	0.01	0.
	0.01	0.01	0.00	0.02	0.02	0.00	0.
$\overline{SK}_T$	-0.39	-0.37	-0.12	-1.24	-0.13	-0.34	-0.
	-0.85	-1.29	-0.49	-2.87	0.17	-0.72	0.
	-0.08	-0.01	0.25	-1.09	-0.22	0.80	-0.
$\bar{G}_T$	1.82	0.95	0.41	1.76	2.78	0.77	2.
	1.53	0.87	0.43	1.74	2.44	1.17	1.
	1.42	0.75	0.44	2.04	2.70	0.52	2.
$\bar{G}_{MIN_T}$	0.05	0.04	0.0	0.03	0.07	0.0	0.
	0.04	0.03	0.0	0.08	0.13	0.0	0.
	0.06	0.02	0.0	0.11	0.14	0.0	0.
$\bar{G}_{MAX_T}$	5.94	3.84	1.96	7.35	8.28	1.75	8.
	6.02	3.96	1.59	6.78	8.65	3.40	9.
	4.39	2.59	1.50	7.11	7.79	1.58	8.
$\bar{L}_T$	-0.01	-0.05	-0.03	-0.13	0.08	0.20	0.
	-0.01	-0.10	-0.09	-0.18	0.11	-0.02	0.
	0.03	0.05	0.07	-0.02	0.09	0.07	0.
$\bar{L}_{MIN_T}$	-12.07	-8.50	-5.75	-14.63	-16.05	-6.00	-16.
	-12.22	-7.89	-5.92	-14.63	-17.79	-9.00	-19.
	-9.65	-7.40	-6.19	-12.43	-14.42	-9.25	-15.
$\bar{L}_{MAX_T}$	12.72	7.15	4.00	11.38	18.92	4.50	19.
	9.54	5.29	3.31	9.17	14.57	9.50	15.
	10.45	6.81	4.03	10.21	17.37	5.00	18.

TABLE VIII(b). Continued from VIII(a).

	All Reports	$\bar{T} \geq 269K$	$\bar{T} \geq 269K$ $S_T < 2K$	$\bar{T} > 269K$ $S_T \geq 2K$	$\bar{T} < 269K$	$\bar{T} < 269K$ $S_T \leq 2K$	$\bar{T} < 269K$ $S_T > 2K$
# cases Div. I	38.	20.	12.	8.	18.	1.	17.
Div. II	13.	9.	6.	3.	7.	1.	6.
Div. III	55.	36.	29.	7.	19.	2.	17.
$\bar{M}_T$	0.58	0.34	0.02	0.83	-0.84	0.22	0.88
	-0.05	0.50	0.33	1.45	-0.77	0.55	-0.99
	0.74	0.38	0.08	1.62	1.43	-0.11	1.61
$\bar{R}_T$	10.54	10.05	9.54	13.81	25.75	7.00	27.74
	13.56	10.28	4.87	23.50	22.36	9.50	24.58
	12.01	8.89	5.66	20.50	21.71	4.75	25.71
$\overline{CFT}_{1\%}$	251.15	272.00	280.75	250.50	240.39	263.00	247.53
	257.59	267.50	275.25	250.00	244.86	263.00	241.83
	264.41	272.50	276.05	257.75	245.08	257.75	243.06
$\overline{CFT}_{16\%}$	266.75	277.13	281.50	260.88	253.22	265.00	254.65
	263.16	273.72	275.42	270.38	249.57	266.00	248.83
	267.92	275.35	277.02	268.50	253.37	259.25	253.24
$\overline{CFT}_{50\%}$	271.55	279.32	282.50	274.44	262.44	267.00	262.13
	268.75	279.50	279.00	274.50	258.14	266.50	350.58
	272.07	277.06	277.31	274.07	262.58	259.75	262.91
$\overline{CFT}_{84\%}$	274.50	280.95	282.17	277.63	267.39	268.50	267.32
	268.22	276.33	275.50	275.82	257.79	270.00	255.75
	274.29	278.31	278.46	276.07	267.24	260.50	268.03
$\overline{CFT}_{99\%}$	277.70	282.70	284.29	276.31	274.14	270.00	272.26
	273.10	277.78	277.92	277.50	267.21	272.00	266.42
	278.42	279.39	279.50	278.25	276.79	262.50	271.76
$\bar{P}_T^1$	0.37	0.38	0.37	0.40	0.35	0.11	0.36
	0.36	0.37	0.39	0.42	0.34	0.00	0.39
	0.35	0.34	0.33	0.38	0.37	0.28	0.38
$\bar{P}_T^2$	0.31	0.33	0.36	0.29	0.28	0.71	0.24
	0.28	0.20	0.15	0.26	0.38	0.81	0.31
	0.30	0.32	0.34	0.26	0.27	0.20	0.25
$\bar{P}_T^3$	0.33	0.28	0.27	0.31	0.37	0.68	0.35
	0.36	0.43	0.50	0.29	0.27	0.19	0.30
	0.35	0.34	0.34	0.30	0.36	0.52	0.35

TABLE VIII(c). Statistical parameters for VIS digital data for N and $N_h \geq .8$, with north-component winds (280° to 090°).

		All Reports	$\bar{T} \geq 269K$	$\bar{T} > 269K$ $S_{\bar{T}} < 2K$	$\bar{T} > 269K$ $S_{\bar{T}} \geq 2K$	$\bar{T} < 269K$	$\bar{T} < 269K$ $S_T \leq 2K$	$\bar{T} < 2$ $S_T >$
# cases	Div. I	38.	20.	12.	8.	18.	1.	17
	Div. II	16.	9.	6.	3.	7.	1.	6
	Div. III	55.	38.	29.	7.	19.	2.	17
$\bar{A}$		128.20	118.32	117.02	107.76	144.74	137.71	145.1
		146.96	139.11	139.16	126.98	162.20	145.12	165.0
		134.89	129.52	129.49	129.64	145.07	140.44	145.6
$\bar{A}_{STA}$		123.08	113.15	117.06	107.38	140.78	135.00	147.4
		140.44	137.00	141.27	118.67	156.57	141.00	161.5
		133.69	132.08	133.24	127.14	142.58	132.00	143.8
$\bar{S}_A$		15.95	15.44	15.16	15.81	12.30	12.20	12.3
		15.13	16.11	15.17	16.01	9.23	8.59	9.4
		14.66	14.90	14.46	16.73	14.20	13.03	14.3
$\overline{CV}_A$		0.14	0.15	0.14	0.15	0.09	0.09	0.0
		0.09	0.12	0.11	0.14	0.06	0.06	0.0
		0.12	0.15	0.12	0.14	0.10	0.10	0.1
$\overline{SK}_A$		-0.19	-0.11	-0.16	-0.04	-0.23	-0.23	-0.2
		-0.40	-0.53	-0.57	-0.43	-0.25	-0.54	-0.2
		-0.37	-0.42	-0.33	-0.70	-0.27	-0.16	-0.2
$\bar{G}_A$		7.72	8.10	8.36	7.74	7.30	8.80	7.3
		7.93	9.81	10.60	8.43	5.51	5.66	5.4
		8.34	8.59	8.34	10.85	8.44	7.20	8.5
$\bar{G}_{MIN_A}$		0.71	0.68	0.66	0.72	0.74	0.71	0.7
		0.51	0.59	0.69	0.37	0.46	0.50	0.4
		0.74	0.82	0.76	1.00	0.60	0.96	0.5
$\bar{G}_{MAX_A}$		21.75	23.28	22.94	25.73	20.07	15.21	20.3
		24.05	27.83	31.49	20.51	16.62	16.38	16.6
		23.51	23.55	22.36	28.58	25.38	17.00	24.1
$\bar{L}_A$		-0.26	-0.27	-0.34	-0.17	-0.24	-1.92	-0.1
		0.45	0.82	1.72	-0.98	-0.04	-1.02	0.1
		-0.47	-0.53	-0.31	-1.71	-0.25	0.36	-0.3
$\bar{L}_{MIN_A}$		-59.93	-56.70	-60.06	-51.75	-56.39	-35.00	-51.8
		-58.81	-66.07	-77.33	-51.33	-46.14	-40.00	-47.1
		-69.24	-70.25	-65.24	-71.00	-67.52	-37.00	-70.8
$\bar{L}_{MAX_A}$		59.95	55.30	61.06	46.75	58.61	37.00	57.7
		65.56	74.33	81.00	61.00	54.14	55.00	54.0
		72.36	73.97	68.06	75.14	71.11	45.00	74.1

TABLE VIII(d). Continued from VIII(c).

	All Reports	$\bar{T} \geq 269K$	$\bar{T} > 269K$ $S_{\bar{T}} < 2K$	$\bar{T} > 269K$ $S_{\bar{T}} \geq 2K$	$\bar{T} < 269K$	$\bar{T} < 269K$ $S_T \leq 2K$	$\bar{T} < 269K$ $S_T > 2K$
# cases Div I	58.	20.	12.	8.	18.	1.	17.
Div II	16.	9.	8.	3.	7.	1.	6.
Div III	55.	36.	29.	7.	19.	2.	17.
	0.95	0.88	1.82	-1.03	1.26	2.29	1.20
M_A	1.41	1.39	1.32	1.02	0.80	0.88	0.79
	1.29	1.34	1.58	1.36	0.83	0.56	0.86
	58.06	61.83	61.00	62.13	53.39	50.00	54.12
$\bar{R}_A$	66.06	66.53	67.33	70.33	48.29	34.00	41.33
	61.31	61.33	54.34	69.57	61.84	58.50	62.24
	98.07	81.45	89.50	70.00	115.44	111.00	115.71
$\overline{CFA}_{1\%}$	123.00	93.07	109.50	66.00	139.56	125.00	142.33
	101.44	96.03	97.54	90.57	111.68	112.00	111.65
	113.95	97.20	100.83	91.75	132.50	124.00	133.06
$\overline{CFA}_{16\%}$	133.12	117.89	124.00	105.67	152.71	136.00	155.50
	119.67	115.75	114.28	121.57	130.89	127.00	131.35
	127.16	114.00	113.83	106.75	140.00	140.00	140.35
$\overline{CFA}_{50\%}$	143.33	137.00	140.50	130.00	150.00	140.00	150.33
	130.18	131.06	131.07	131.00	149.89	141.00	146.47
	142.29	129.20	132.17	124.75	156.83	150.00	157.24
$\overline{CFA}_{84\%}$	159.44	150.33	153.17	144.67	171.14	156.00	174.17
	147.39	149.44	144.00	146.29	160.00	153.50	160.82
	155.08	145.30	147.50	142.00	169.33	161.00	169.82
$\overline{CFA}_{99\%}$	171.00	164.00	167.83	156.33	180.14	156.00	184.07
	162.95	157.50	156.67	160.14	173.53	170.50	175.88
	0.35	0.39	0.42	0.35	0.31	0.06	0.33
$\bar{P}_A^1$	0.28	0.26	0.30	0.19	0.30	0.31	0.30
	0.25	0.27	0.28	0.24	0.32	0.36	0.31
	0.27	0.25	0.24	0.34	0.26	0.12	0.27
$\bar{P}_A^2$	0.32	0.27	0.24	0.23	0.43	0.20	0.47
	0.26	0.27	0.30	0.27	0.26	0.14	0.27
	0.38	0.34	0.34	0.33	0.43	0.53	0.40
$\bar{P}_A^3$	0.40	0.39	0.46	0.38	0.26	0.49	0.33
	0.43	0.43	0.42	0.49	0.42	0.48	0.42

TABLE IX. Comparison of fog and no-fog statistical parameters for the following temperature categories: $\bar{T} \geq 269K$ with $S_T \leq 2K$; $\bar{T} \geq 269K$ with $S_T > 2K$; and $\bar{T} < 269K$ with $S_T > 2K$. Differences are calculated for stratifications with $N \geq .8$, $N_h \geq .8$ with south winds and $N_H \geq .8$ with north winds. a) IR Difference = DIV I - DIV III

	$\bar{T} > 269K$ $S_T \leq 2K$		$\bar{T} \geq 269K$ $S_T > 2K$		$\bar{T} < 269K$ $S_T > 2K$		
%(number)	44(57)	58(43)	52(25)	63(15)	35(69)	37(51)	DIV I
of cases	39(50)	23(17)	33(16)	21(5)	46(91)	42(59)	DIV III
	45(55)	26(12)	57(25)	44(8)	38(69)	43(17)	DIV I
	38(46)	61(29)	27(12)	39(7)	43(79)	43(17)	DIV III
$\bar{\bar{T}}$	3.4	3.3	1.8	2.2	0.3	0.1	
	3.3	4.8	2.4	1.2	0.3	0.0	
$\bar{T}_{STA}$	3.4	3.4	1.6	2.2	0.4	0.1	
	3.4	5.0	1.9	-0.1	0.4	0.1	
$\bar{S}_T$	-0.1	-0.2	-0.3	0.3	0.8	1.0	
	-0.1	0.0	-0.2	-0.2	0.7	-0.2	
$\overline{CV}_T$	0.0	0.0	0.0	0.0	0.0	0.0	
	0.0	0.0	0.0	0.0	0.0	0.0	
$\overline{SK}_T$	-0.2	0.1	-0.6	-0.5	0.1	-0.1	
	-0.2	-0.4	-0.4	-0.2	0.0	0.2	
$\bar{G}_T$	0.0	-0.1	0.2	-0.1	0.2	0.4	
	-0.1	0.0	-0.3	-0.3	0.2	-0.1	
$\bar{G}_{MIN_T}$	0.0	0.0	0.0	0.0	0.0	0.1	
	0.0	0.0	0.0	0.0	0.0	-0.1	
$\bar{G}_{MAX_T}$	-0.1	-0.3	0.1	-0.2	1.3	1.7	
	-0.1	0.0	-0.4	0.2	1.2	0.2	
$\bar{\bar{L}}_T$	0.0	0.0	0.2	-0.2	0.0	0.0	
	0.0	-0.1	-0.2	-0.1	0.0	0.0	
$\bar{L}_{MIN_T}$	0.3	0.5	0.3	0.9	-1.3	-1.3	
	0.4	0.4	1.0	-0.2	-1.1	-1.6	
$\bar{L}_{MAX_T}$	-0.9	-1.9	-3.4	-2.2	1.9	2.2	
	-0.8	-0.1	-4.9	-6.3	1.7	0.9	
$\bar{M}_T$	0.0	0.0	-0.1	0.5	-0.1	-0.2	
	0.0	-0.1	-0.1	-0.8	-0.2	-0.7	
$\bar{R}_T$	-0.4	-1.2	-0.1	3.3	2.8	3.5	
	-0.5	-0.1	-0.2	-0.7	2.5	1.0	
$\overline{CFT}_{1\%}$	3.5	4.1	1.4	-1.3	-1.8	-2.1	
	3.5	4.7	2.4	2.7	-1.4	-0.5	
$\overline{CFT}_{16\%}$	3.5	3.4	2.3	1.9	-0.2	-0.8	
	3.4	4.9	2.6	1.5	0.0	1.4	
$\overline{CFT}_{50\%}$	3.3	3.3	1.7	2.7	0.2	0.0	
	3.2	4.8	2.2	0.4	0.1	0.0	
$\overline{CFT}_{84\%}$	3.2	3.1	1.4	2.0	1.1	1.3	
	3.1	4.7	2.2	1.6	1.0	-0.7	
$\overline{CFT}_{99\%}$	3.1	2.9	1.3	2.0	1.1	1.3	
	3.0	4.6	2.2	2.0	1.1	0.5	
$\bar{P}_T^1$	0.0	0.0	0.0	0.0	-0.1	0.0	
	0.0	0.0	0.0	0.0	0.0	0.0	
$\bar{P}_T^2$	0.0	0.0	0.1	0.2	0.0	0.0	
	0.0	0.0	0.1	0.0	0.0	0.0	
$\bar{P}_T^3$	0.0	0.0	-0.1	0.0	0.0	0.1	
	0.0	-0.1	-0.1	0.0	0.0	0.0	

TABLE IX. (Continued)

KEY: $N_{8,9}$ | $So, N_{h_{8,9}}$ / $N_{h_{8,9}}$ | $No, N_{h_{8,9}}$

b) VIS Difference = DIV I - DIV III

	$\bar{T} \geq 269K$ $S_T \leq 2K$		$\bar{T} \geq 269K$ $S_T > 2K$		$\bar{T} < 269K$ $S_T > 2K$		
%(number) of cases	44(57)	58(43)	52(25)	63(15)	35(69)	37(51)	DIV I
	39(50)	23(17)	33(16)	21(5)	46(91)	42(59)	DIV III
	45(55)	26(12)	57(25)	44(8)	38(69)	43(17)	DIV I
	38(46)	61(29)	27(12)	39(7)	43(79)	43(17)	DIV III
$\bar{A}$	-13.5	-14.9	-7.9	-12.5	-5.1	-7.6	
	-12.6	-12.5	-12.0	-21.9	-5.4	-0.5	
A_{STA}	-16.3	-17.3	-12.9	-19.9	-3.6	-7.4	
	-14.5	-16.2	-15.3	-19.8	-4.1	3.7	
$\bar{S}_A$	-0.6	-1.8	-2.1	0.4	-0.3	0.6	
	-0.6	0.7	-1.1	-0.9	-0.1	-2.0	
$\overline{CV}_A$	0.0	0.0	0.0	0.0	0.0	0.0	
	0.0	0.0	0.0	0.0	0.0	0.0	
$\overline{SK}_A$	0.4	0.5	0.3	0.3	0.0	0.0	
	0.3	0.2	0.9	0.7	0.0	0.0	
$\bar{G}_A$	-0.2	-0.8	-2.5	-0.7	-0.7	-0.3	
	-0.1	0.3	-2.0	-0.3	-0.6	-1.3	
$\bar{G}_{MIN_A}$	-0.1	-0.1	-0.1	-0.2	0.0	0.0	
	-0.1	-0.1	-0.2	-0.3	0.0	0.2	
$\bar{G}_{MAX_A}$	-0.3	-2.5	-4.2	0.3	-1.7	-0.1	
	0.2	0.6	-3.0	-4.9	-1.3	-3.8	
$\bar{L}_A$	-0.2	-0.4	1.1	0.1	-0.1	-0.3	
	0.0	0.0	1.0	1.5	-0.2	0.2	
$\bar{L}_{MIN_A}$	3.9	-0.5	38.7	17.9	8.8	4.9	
	1.3	5.2	28.5	39.3	8.6	19.1	
$\bar{L}_{MAX_A}$	-12.7	-11.9	-30.1	-5.7	-10.6	-6.1	
	-7.3	-7.8	-25.9	-48.4	-9.0	-16.4	
$\bar{M}_A$	-0.8	-0.9	-0.9	-0.9	0.1	0.2	
	-0.6	0.2	-1.3	-0.3	0.3	-0.3	
$\bar{R}_A$	-2.7	-6.8	-8.5	-0.9	-3.3	-0.1	
	-1.7	1.7	-5.4	-6.4	-2.6	-8.1	
$\overline{CFA}_{1\%}$	-8.5	-6.6	-1.1	-9.9	-3.3	-8.2	
	-8.8	-10.8	-5.1	-11.7	-4.4	4.1	
$\overline{CFA}_{16\%}$	-13.4	-12.9	-5.1	-13.3	-4.9	-8.2	
	-12.1	-13.5	-10.7	-19.8	-5.3	1.7	
$\overline{CFA}_{50\%}$	-14.3	-16.5	-8.8	-13.4	-5.0	-7.3	
	-13.2	-12.2	-13.0	-24.3	-5.1	-0.1	
$\overline{CFA}_{84\%}$	-13.9	-16.2	-10.0	-12.2	-5.4	-6.7	
	-13.1	-11.9	-12.7	-21.5	-5.6	-3.6	
$\overline{CFA}_{99\%}$	-11.3	-13.4	-9.5	-10.7	-6.6	-8.2	
	-10.5	-9.2	-10.5	-13.1	-7.0	-4.1	
$\bar{P}_A^1$	0.0	0.0	0.0	0.0	0.0	0.0	
	0.1	0.1	0.1	0.1	0.0	0.0	
$\bar{P}_A^2$	0.0	0.0	0.0	-0.1	0.0	0.0	
	0.0	-0.1	0.0	0.1	0.0	0.0	
$\bar{P}_A^3$	0.0	0.0	0.0	0.0	0.0	0.0	
	0.0	-0.1	-0.1	-0.2	0.0	0.0	

TABLE X. Comparison of fog and no-fog statistical parameter differences for FLCG1-FLCG7 versus differences for FLCG1&2-FLCG7 for same temperature categories as Table IX.

a) IR Difference = DIV I - DIV III

	$\bar{T} > 269K$ $S_T \leq 2K$		$\bar{T} > 269K$ $S_T > 2K$		$\bar{T} < 269K$ $S_T > 2K$		
%(number) of cases	45(48)	58(43)	63(15)	63(15)	44(61)	37(51)	FLCG1,2 DI
	23(17)	23(17)	21(5)	21(5)	42(59)	42(59)	DIV III DI
	34(16)	26(12)	50(9)	44(8)	43(17)	43(17)	FLCG1,2 DI
	62(29)	62(29)	39(7)	39(7)	43(17)	43(17)	DIV III DI
$\bar{\bar{T}}$	-3.0	3.3	2.2	2.2	0.2	0.1	
	2.7	4.8	1.3	1.2	0.0	0.0	
$\bar{T}_{STA}$	-3.1	3.4	2.5	2.2	-0.3	0.1	
	0.9	5.0	0.1	-0.1	0.1	0.1	
$\bar{S}_T$	-0.2	-0.2	0.3	0.3	0.9	1.0	
	0.1	0.0	-0.3	-0.2	-0.2	-0.2	
$\overline{CV}_T$	0.0	0.0	0.0	0.0	0.0	0.0	
	0.0	0.0	0.0	0.0	0.0	0.0	
$\overline{SK}_T$	0.1	0.1	-0.5	-0.5	-0.1	-0.1	
	-0.5	-0.4	-0.7	-0.2	0.2	0.2	
$\bar{G}_T$	-0.4	-0.1	-0.1	-0.1	0.3	0.4	
	0.0	0.0	-0.4	-0.3	-0.1	-0.1	
$\bar{G}_{MIN_T}$	0.0	0.0	0.0	0.0	0.0	0.1	
	0.0	0.0	0.0	0.0	-0.1	-0.1	
$\bar{G}_{MAX_T}$	-0.3	-0.3	-0.2	-0.2	1.5	1.7	
	0.1	0.0	0.8	0.2	0.2	0.2	
$\bar{\bar{L}}_T$	0.0	0.0	-0.3	-0.2	0.1	0.0	
	-0.1	-0.1	-0.1	-0.1	0.0	0.0	
$\bar{L}_{MIN_T}$	0.6	0.5	-0.9	0.9	-1.0	-1.3	
	0.1	0.4	-0.1	-0.2	-1.6	-1.6	
$\bar{L}_{MAX_T}$	-1.7	-1.9	-2.2	-2.2	1.8	2.2	
	-0.1	-0.1	-7.2	-6.3	0.9	0.9	
$\bar{M}_T$	0.0	0.0	0.5	0.5	-0.1	-0.2	
	0.0	-0.1	-0.8	-0.8	-0.7	-0.7	
$\bar{R}_T$	-1.2	-1.2	3.3	3.3	3.0	3.5	
	0.3	-0.1	0.5	-0.7	1.0	1.0	
$\overline{CFT}_{1\%}$	3.7	4.1	-1.3	-1.3	-1.8	-2.1	
	2.2	4.7	1.3	2.7	-0.5	-0.5	
$\overline{CFT}_{16\%}$	3.1	3.4	1.9	1.9	-0.7	-0.8	
	2.8	4.9	2.1	1.5	1.4	1.4	
$\overline{CFT}_{50\%}$	2.9	3.3	2.7	2.7	0.1	0.0	
	2.7	4.8	0.5	0.4	-0.1	0.0	
$\overline{CFT}_{84\%}$	2.8	3.1	2.0	2.0	1.3	1.3	
	2.5	4.7	1.4	1.6	-0.7	-0.7	
$\overline{CFT}_{99\%}$	2.5	2.9	2.0	2.0	1.2	1.3	
	2.6	4.6	1.8	2.0	0.5	0.5	
$\bar{P}_T^1$	0.0	0.0	0.0	0.0	0.0	0.0	
	0.0	0.0	0.0	0.0	0.0	0.0	
$\bar{P}_T^2$	0.0	0.0	0.2	0.2	0.0	0.0	
	0.0	0.0	0.0	0.0	0.0	0.0	
$\bar{P}_T^3$	0.0	0.0	-0.2	0.0	0.0	0.1	
	0.0	-0.1	0.0	0.0	0.0	0.0	

TABLE X. (Continued)

KEY:

$So, N_{h_{8,9}}$ FLCG1&2-7	$So, N_{h_{8,9}}$ FLCG1-7
$No, N_{h_{8,9}}$ FLCG1&2-7	$No, N_{h_{8,9}}$ FLCG1-7

b) VIS Difference = DIV I - DIV III

	$\bar{T} > 269K$ $S_{\bar{T}} \leq 2K$		$\bar{T} > 269K$ $S_{\bar{T}} > 2K$		$\bar{T} < 269K$ $S_T > 2K$		
%(number)	65(48)	58(43)	63(15)	63(15)	44(61)	37(51)	FLCG1,2 DIV I
of cases	23(17)	23(17)	21(5)	21(5)	42(59)	42(59)	DIV III DIV III
	34(16)	26(12)	50(9)	44(8)	43(17)	43(17)	FLCG1,2 DIV I
	62(29)	62(29)	39(7)	39(7)	43(17)	43(17)	DIV III DIV III
$\bar{A}$	-12.6	-14.9	-12.5	-12.5	-5.9	-7.6	
	-6.7	-12.5	-21.2	-21.9	-0.5	-0.5	
$\bar{A}_{STA}$	-14.7	-17.3	-19.9	-19.9	-6.5	-7.4	
	-9.8	-16.2	-18.4	-19.8	3.7	3.7	
$\bar{S}_A$	-2.3	-1.8	0.4	0.4	0.4	0.6	
	1.0	0.7	-0.2	-0.9	-2.0	-2.0	
$\overline{CV}_A$	0.0	0.0	0.0	0.0	0.0	0.0	
	0.0	0.0	0.0	0.0	0.0	0.0	
$\overline{SK}_A$	0.5	0.5	0.3	0.3	2.0	0.2	
	0.1	0.2	0.6	0.7	0.0	0.0	
$\bar{G}_A$	-1.0	-0.8	-0.7	-0.7	-0.3	-0.3	
	1.0	0.3	-2.8	-0.3	-1.3	-1.3	
$\bar{G}_{MIN_A}$	-0.1	-0.1	-0.2	-0.2	0.0	0.0	
	-0.1	-0.1	-0.3	-0.3	0.2	0.2	
$\bar{G}_{MAX_A}$	-3.3	-2.5	-0.3	0.3	-0.4	-0.1	
	3.4	0.6	-4.3	-4.9	-3.8	-3.8	
$\bar{L}_A$	-0.5	-0.4	0.1	0.1	-0.3	-0.3	
	0.5	0.0	1.5	1.5	0.2	0.2	
$\bar{L}_{MIN_A}$	1.0	-0.5	17.9	17.9	4.8	4.9	
	-0.7	5.2	39.0	39.3	-19.1	19.1	
$\bar{L}_{MAX_A}$	-12.7	-11.9	-5.7	-5.7	-6.7	-6.1	
	-2.1	-7.8	-44.0	-48.4	-16.4	-16.4	
$\bar{M}_A$	-1.6	-0.9	-0.9	-0.9	-0.1	0.2	
	0.1	0.2	-1.8	-0.3	0.3	-0.3	
$\bar{R}_A$	-8.3	-6.8	-0.8	-0.9	-0.5	-0.1	
	4.0	1.7	-4.4	-6.4	-8.1	-8.1	
$\overline{CFA}_{1\%}$	-3.6	-6.6	-9.9	-9.9	-5.9	-8.2	
	-7.3	-10.8	-12.6	-11.7	4.1	4.1	
$\overline{CFA}_{16\%}$	-10.0	-12.9	-13.3	-13.3	-6.3	-8.2	
	-7.8	-13.5	-20.6	-19.8	1.7	1.7	
$\overline{CFA}_{50\%}$	-14.2	-16.5	-13.4	-13.4	-5.8	-7.3	
	-6.6	-12.2	-23.0	-24.3	-0.1	-0.1	
$\overline{CFA}_{84\%}$	-14.3	-16.2	-12.2	-12.2	-5.1	-6.7	
	-16.1	-11.9	-20.4	-21.5	-3.6	-3.6	
$\overline{CFA}_{99\%}$	-11.9	-13.4	-10.7	-10.7	-6.4	-8.2	
	-3.4	-9.2	-16.9	-18.1	-4.1	-4.1	
$\bar{P}_A^1$	0.0	0.0	0.0	0.0	0.0	0.0	
	0.1	0.1	0.1	0.1	0.0	0.0	
$\bar{P}_A^2$	0.0	0.0	-0.1	-0.1	0.0	0.0	
	-0.3	-0.1	0.0	0.1	0.0	0.0	
$\bar{P}_A^3$	0.0	0.0	0.0	0.0	0.0	0.0	
	0.0	-0.1	-0.1	-0.2	0.0	0.0	

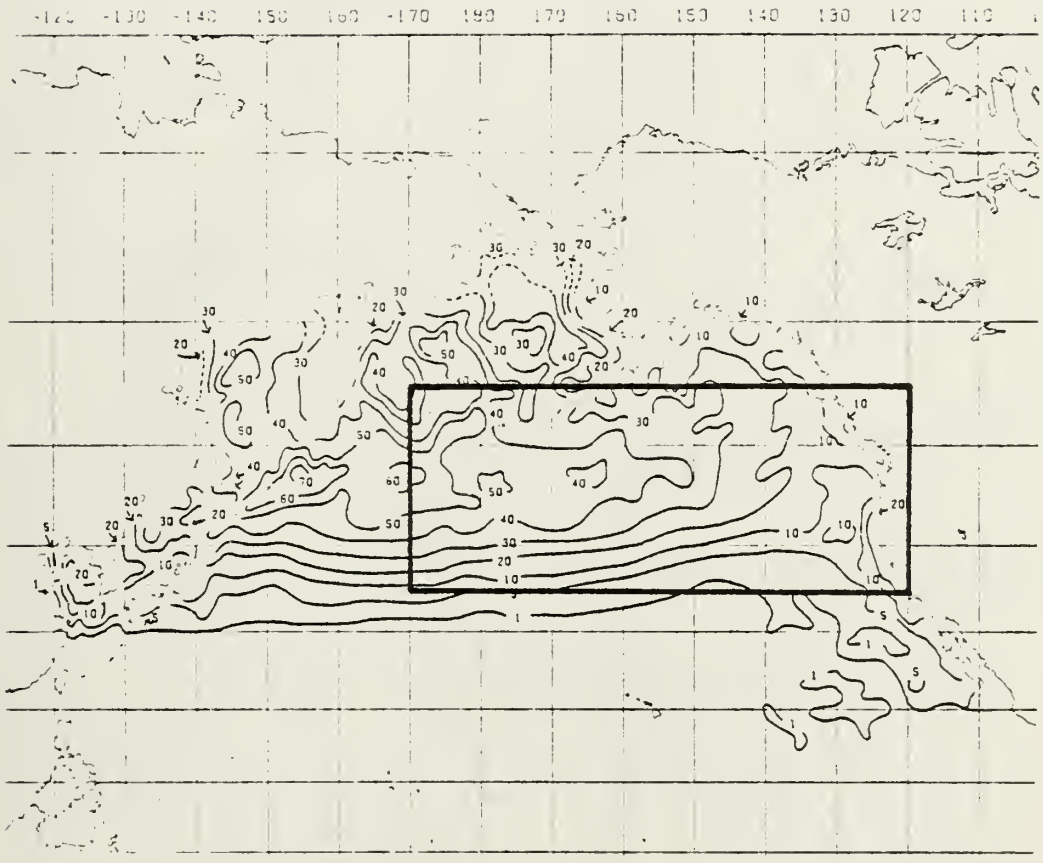

Figure 1. Area of study (enclosed area) and July climatological marine-fog frequencies (%) (U.S. Navy, Naval Oceanography and Meteorology, 1978).

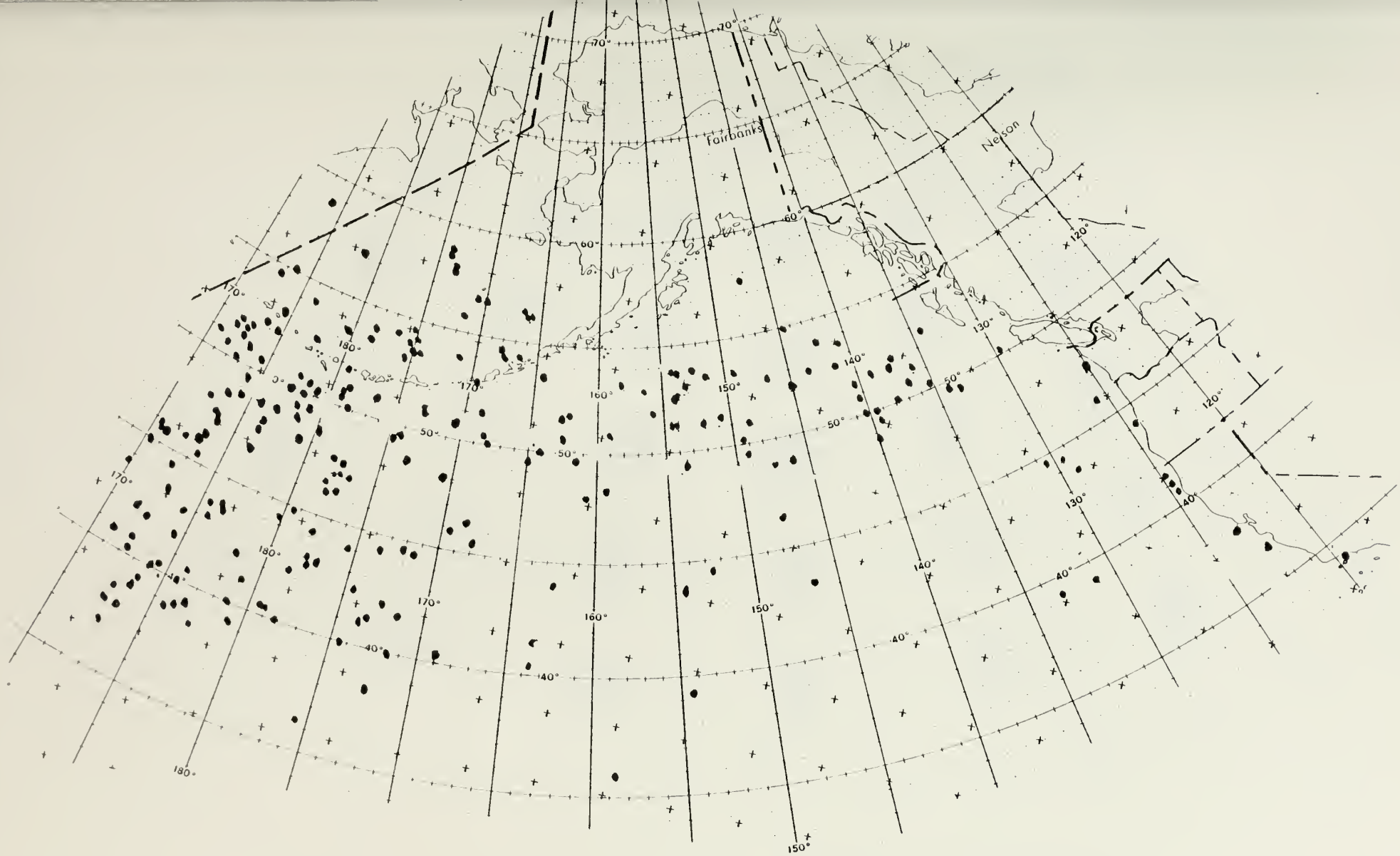

Figure 2. Locations of 248 ground-truth observations for FLCG1 through 6 (0000 GMT 28, 29 June, 1, 2, 3, 5, 6, 14 July 1978).

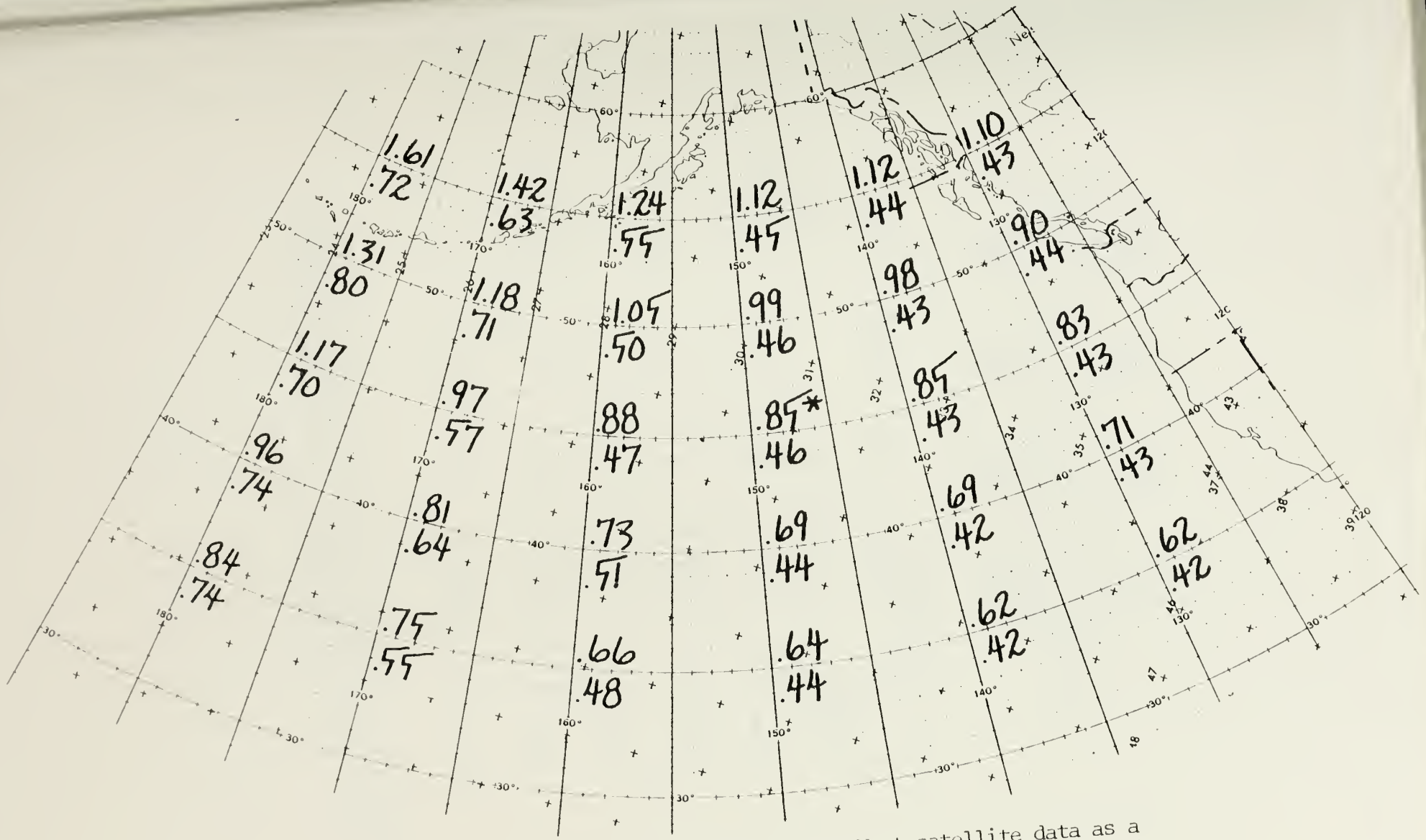

Figure 3. Line and element spacing (nmi) of GOES-West satellite data as a function of latitude and longitude position (sample at 2345 GMT 3 July 1978). Values are approximate only due to computational processing.

*estimated value

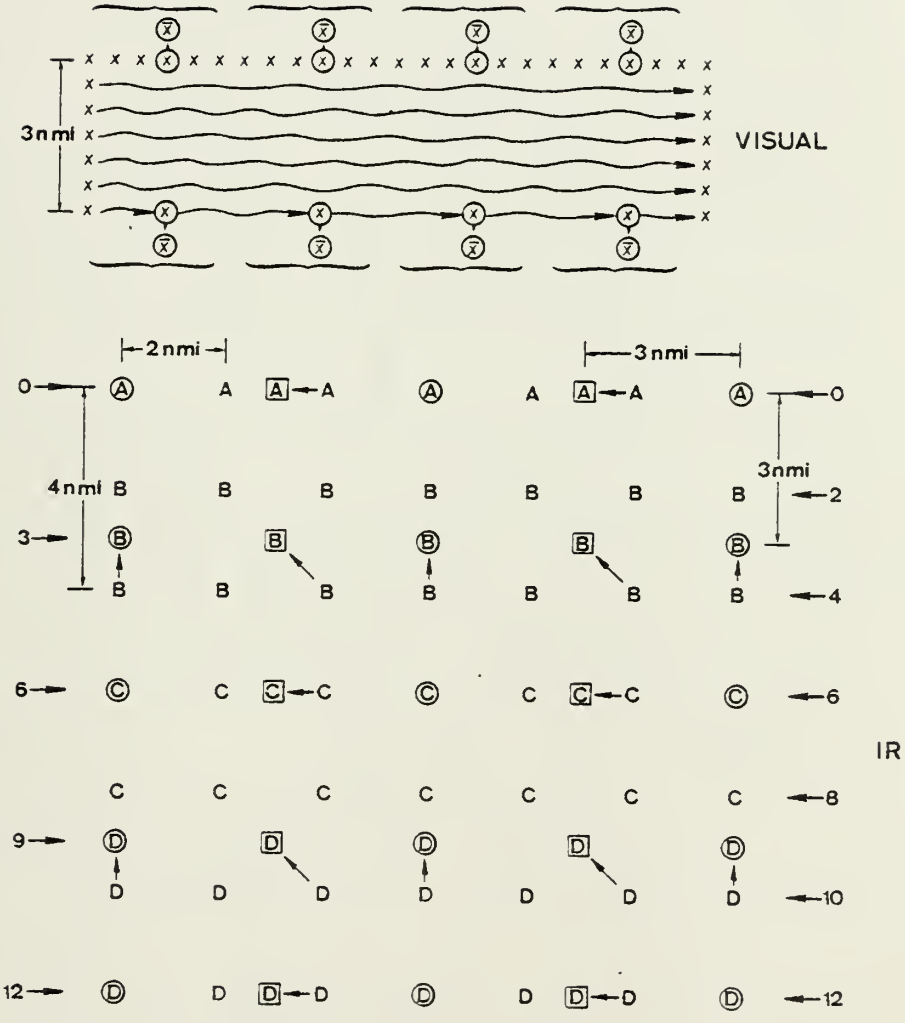

Figure 4. Scheme for selection of full resolution IR and VIS GOES-West satellite data to fulfill 3 nmi x 3 nmi data criterion. For VIS, (x̄) values used; for IR ○ and □ values used.

149621	682	0	0	0	0	682	0	0	0	0	0	0	0	0	0
0	0	0	0	341	0	0	0	2	0	2	16	59	42	69	174
315	239	199	212	340	213	243	0	461	622	369	307	416	809	558	591
786	1207	0	760	682	970	1297	829	688	1503	0	1754	1171	841	1303	2064
1529	0	1413	1857	2887	1879	1754	0	2101	3474	2534	2166	3603	0	5053	3360
3406	0	4059	5787	4774	5084	0	8371	13056	10642	0	8353	9786	13462	0	10576
10327	17230	0	16946	11093	7865	0	8179	10749	0	7245	6589	10061	0	13148	8419
0	7810	9164	0	11417	8263	0	7246	11031	0	13321	6244	0	4359	4984	0
6480	0	3796	3356	0	4223	5898	0	3348	0	3095	3593	0	4787	0	2485
2356	0	3236	0	4392	0	2362	0	2183	2711	0	3931	0	2088	0	2042
0	2531	0	3644	0	1835	0	1799	0	2238	0	3247	0	1700	0	1773
2205	3230	0	1668	1550	1894	2793	1568	1566	2032	0	2787	1592	1684	1987	0
2370	1756	1742	0	2075	2137	0	1434	1133	0	1037	729	0	412	292	0
335	0	526	0	821	0	350	0	371	0	474	0	409	0	229	0
341	176	682	179	0	0	55	0	0	27	0	0	105	0	0	0
247	0	0	81	0	0	0	0	170	0	0	0	0	287	56103	0

Figure 5. Frequency distribution of IR DCV distribution for data frame time 2345 GMT 27 June 1978. DCV of zero (255) is represented by upper left (lower right) corner square.

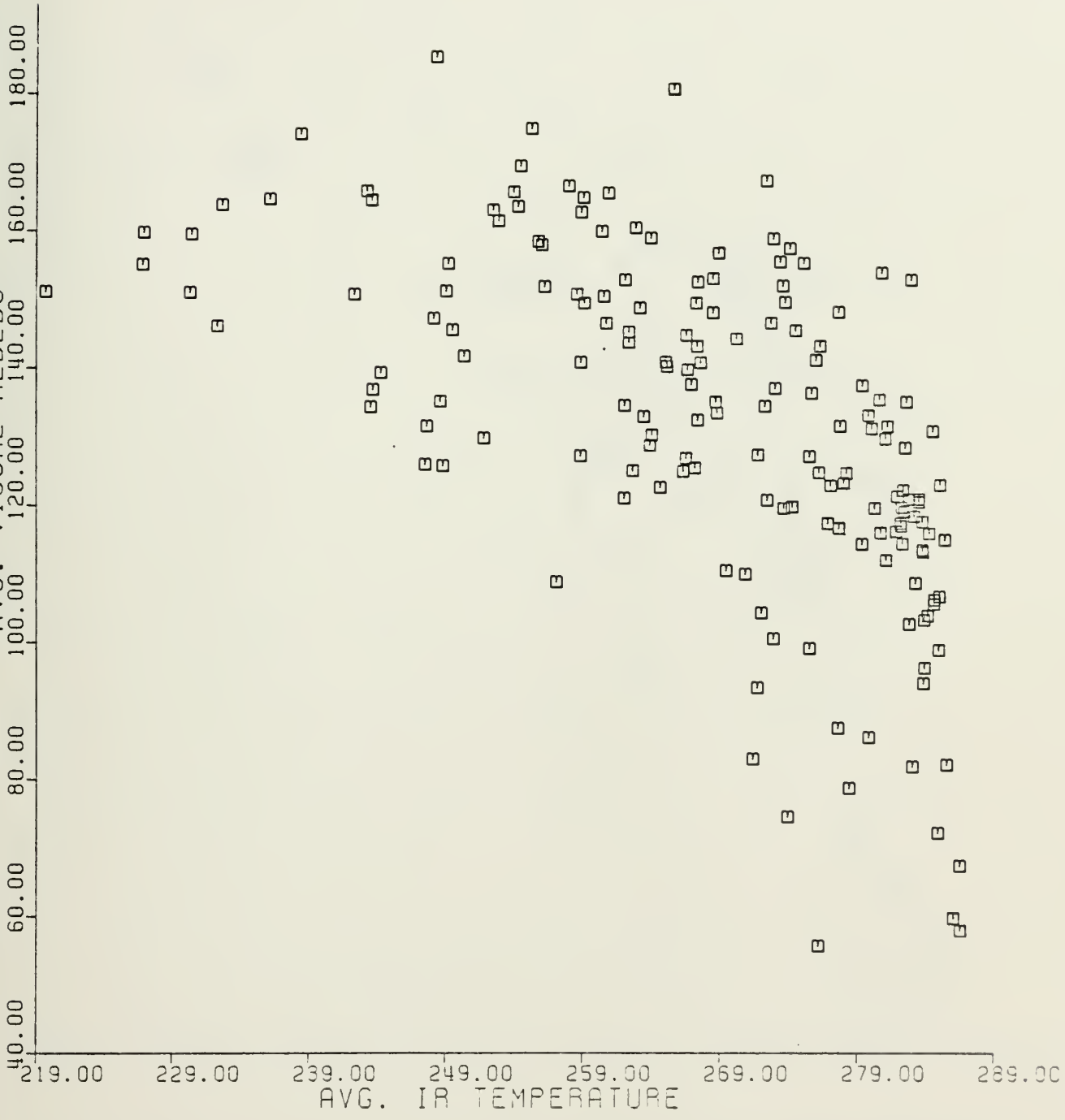

Figure 6(a). Comparison of average IR temperature vs average VIS DCV for fog observations (FLC1), no temperature restriction.

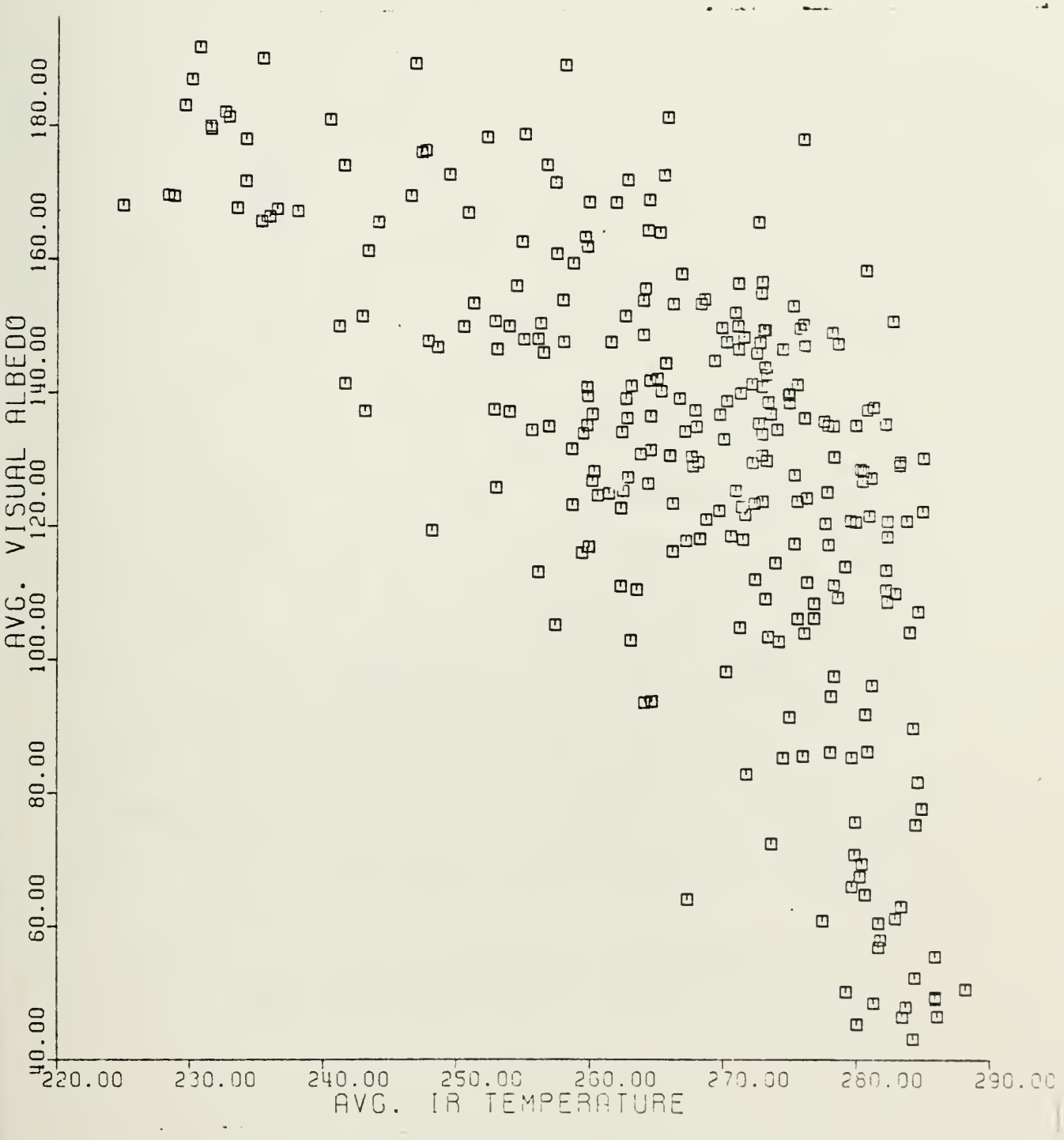

Figure 6(b). Comparison of average IR temperature vs average VIS DCV for no-fog (FLC7) observations, no temperature restriction.

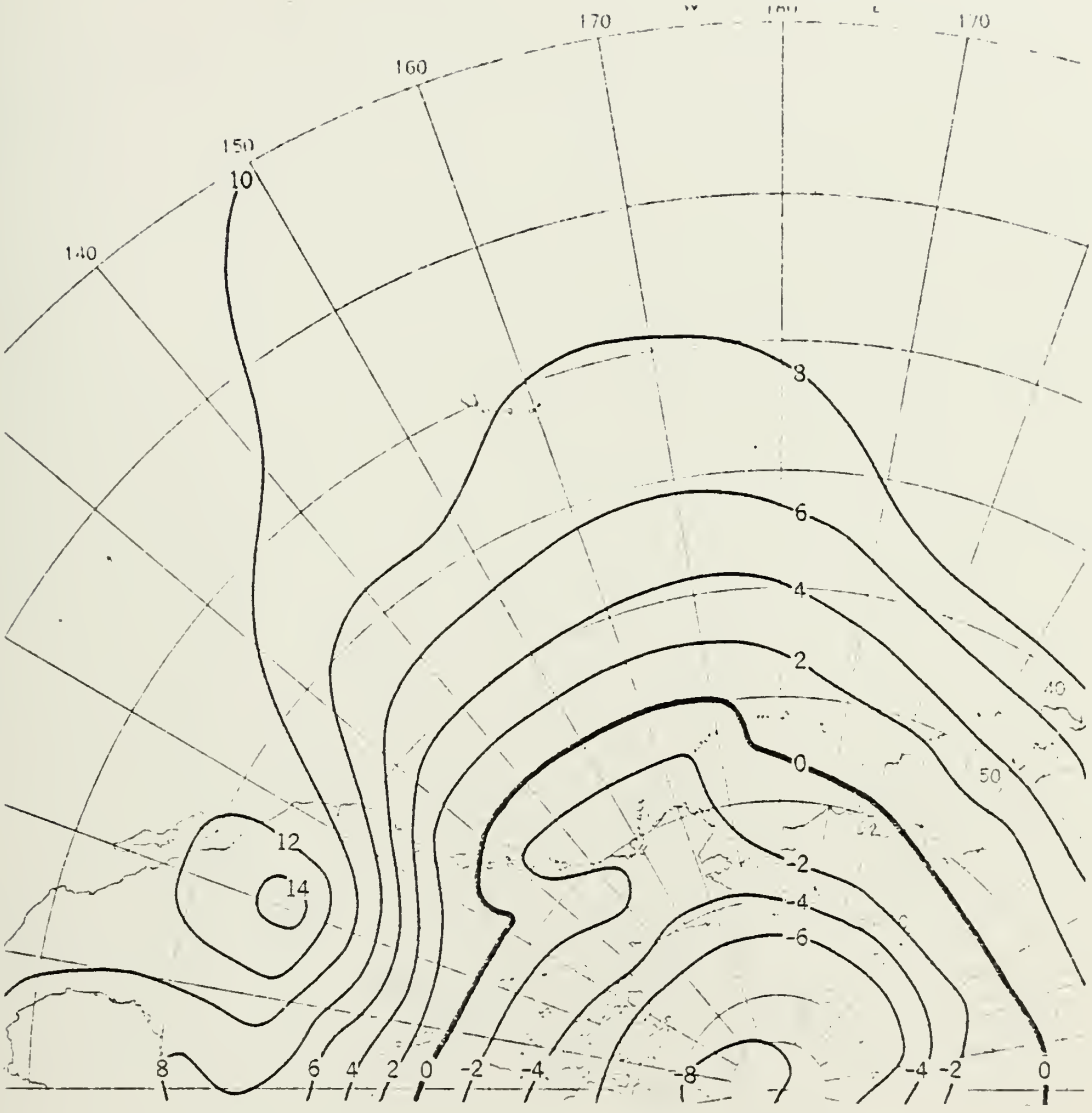

Figure 7. July 700 kPa climatological temperatures (°C) (U.S. Navy, Naval Weather Service Command, 1970).

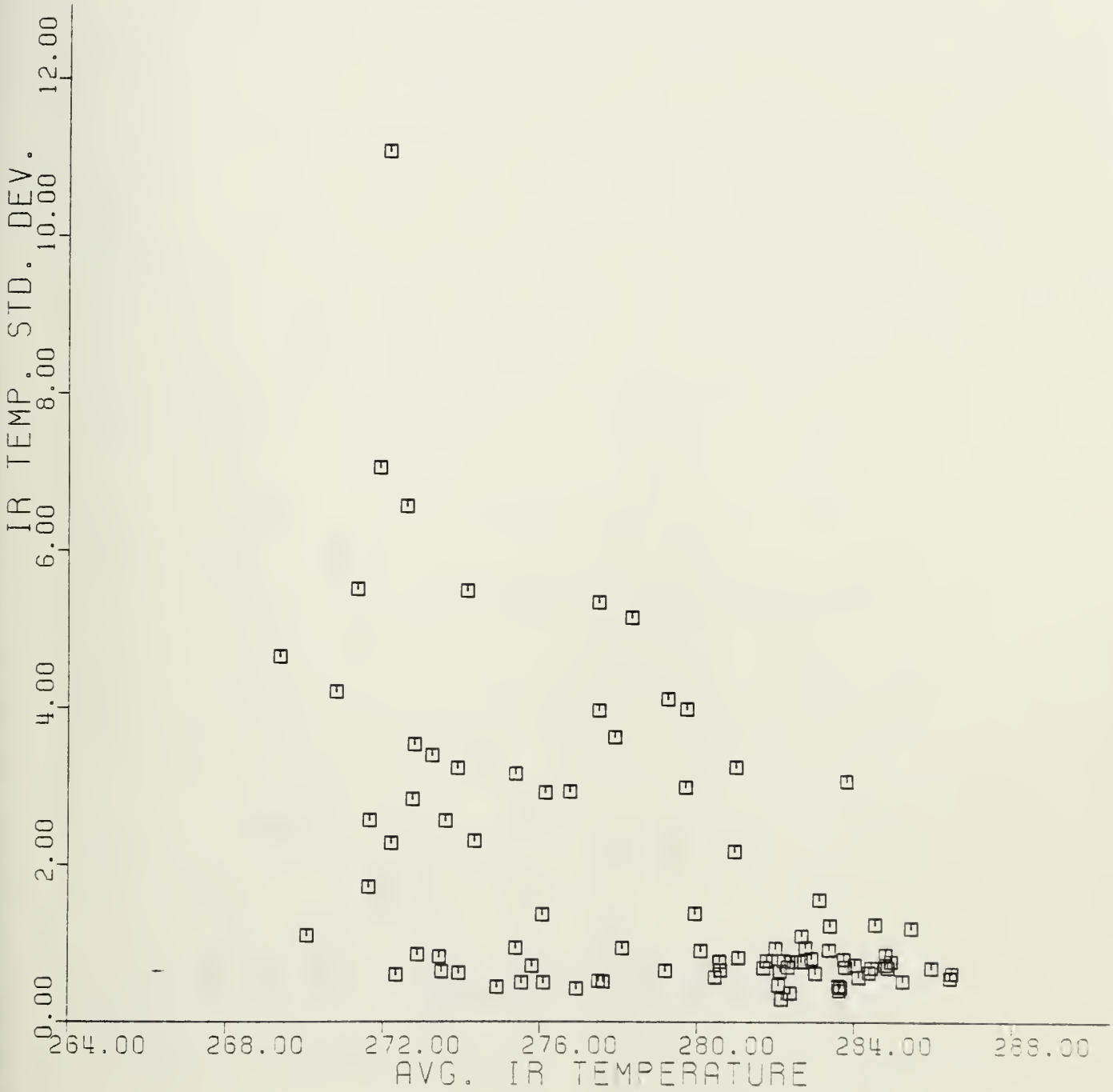

Figure 8(a). Comparison of average IR temperature vs standard deviation of IR temperatures for fog observations (FLC1), restricted to $T \geq 269$ K.

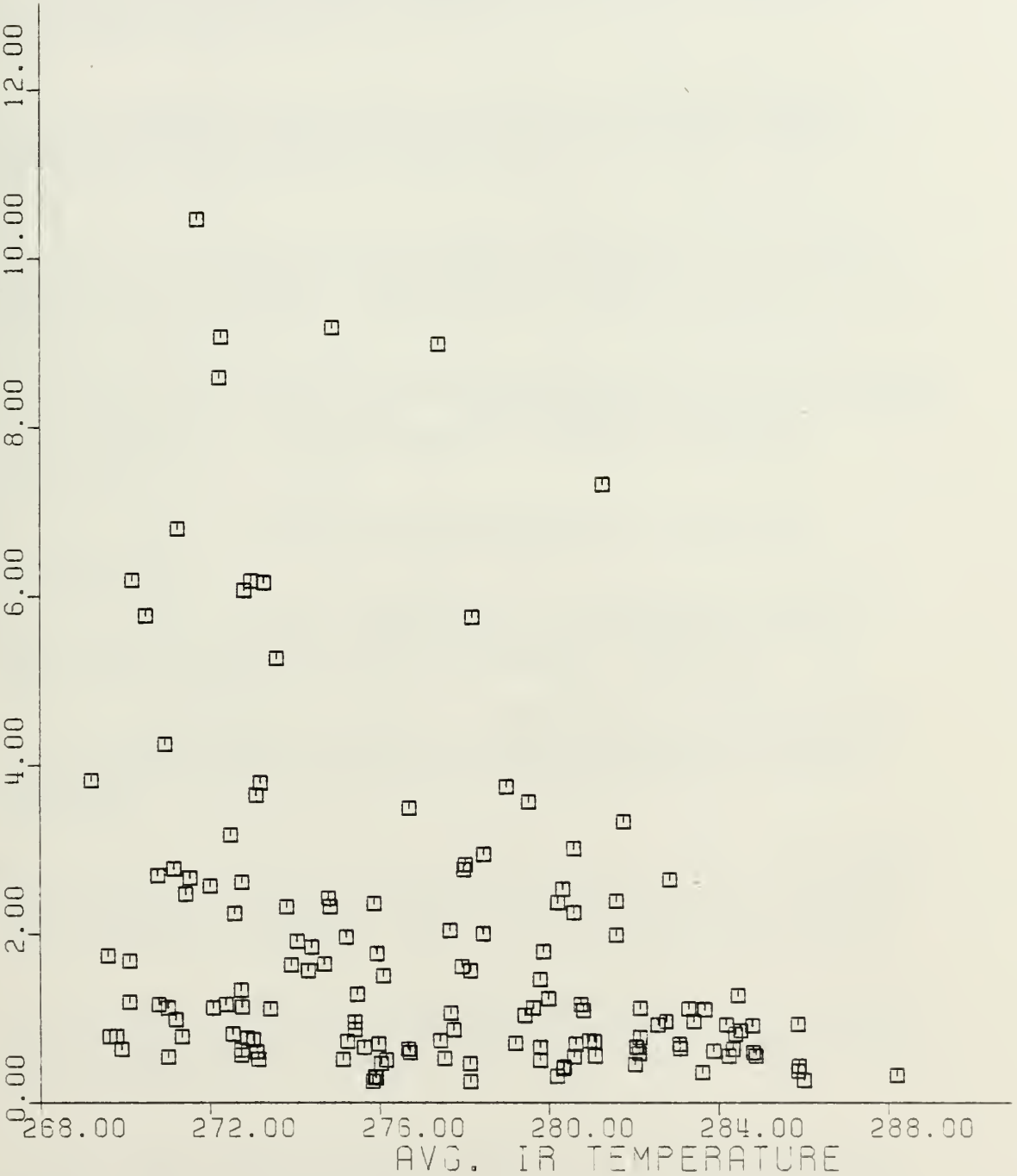

Figure 8(b). Comparison of average IR temperature vs standard deviation of IR temperatures for no-fog observations (FLC7), restricted to $T \geq 269$ K.

LIST OF REFERENCES

Booth, A. L., 1973: Objective Cloud Type Classification Using Visual and Infrared Satellite Data. Technical Note BN 768, Institute for Fluid Dynamics and Applied Mathematics, University of Maryland, 62 pp.

Hale, R. E. and Renard, R. J., 1975: Use of the NOAA-2 Digitized Satellite Data for Diagnosing Marine Fog in the North Pacific Ocean Area. NPS-51HI75091, Naval Postgraduate School, Monterey, California, 92 pp.

Ihli, C. B., Jr. and Renard, R. J., 1977: The Use of DMSP and SMS-2 Digital Satellite Data for Identifying Marine Fog in the Eastern North Pacific Ocean Area. NPS-63Ih77031, Naval Postgraduate School, Monterey, California, 99 pp.

National Oceanic and Atmospheric Administration and National Aeronautics and Space Administration, 1976: The GOES/SMS User's Guide. Editors: R. P. Corbell, C. J. Callahan and W. J. Kotsch, NOAA/NASA, Washington, D. C., 118 pp.

Quayle, R. G., 1976: Weather and Maritime Casualty Statistics. Mar. Wea. Log, Vol. 20, No. 2, pp. 74-80.

Quinn, P. F., 1978: Further Development of a Statistical Diagnostic Model of Marine Fog Using FNWC Model Output Parameters. M. S. Thesis Naval Postgraduate School, Monterey, California, 73 pp.

Renard, R. J. and Servaas, T., 1977: Climatological Fog Frequencies as a Function of Wind Direction and Speed, Unpublished research, Department of Meteorology, Naval Postgraduate School, Monterey, California.

Stevenson, M. R., Kirkham, R. G. and Madsen, B. J., 1977: Development and Testing of a Cloud Screening Technique for Use with Satellite-borne Scanning Radiometers. NEPRF Cont.No.N0028-76-C-3163, Inter-American Tuna Com., Scripps Inst. of Oceg., La Jolla, CA, 95 pp.

U. S. Navy, Naval Oceanography and Meteorology, 1978: Study of World-wide Occurrence of Fog, Thunderstorms, Supercooled Low Clouds and Freezing Temperatures (NAVAIR 50-1C-60CHI). NWSED, Federal Building, Asheville, N.C.

U. S. Navy, Naval Weather Service Command, 1970: Selected Level Heights, Temperatures and Dew Points for the Northern Hemisphere (NAVAIR 50-1C-52). Superintendent of Documents, U.S. Government Printing Office, Washington, D.C.

U. S. Navy, Naval Weather Service Command, 1975: Numerical Environmental Products Manual, NAVAIR 50-1G-522.

Van Orman, B. L. and Renard, R. J., 1977: Statistical Diagnostic Modelling of Marine Fog Using Model Output Parameters. M. S. Thesis, Department of Meteorology, Naval Postgraduate School, Monterey, California, 94 pp.

Wallace, R. T. and Renard R. J., 1975: The Use of Meteorological Satellites for Discerning Marine Fog. NPS-51Wa75031, Naval Postgraduate School, Monterey, California, 59 pp.

Wheeler, S. E. and Leipper, D. F., 1974: Marine Fog Impact on Naval Operations. NPS Report 58Wh74091, Department of Oceanography, Naval Postgraduate School, Monterey, California, 118 pp.

Willms, G. P., 1975: A Climatology of Marine-Fog Frequencies for the North Pacific Ocean Summer Fog Season. M. S. Thesis, Department of Meteorology, Naval Postgraduate School, Monterey, California, 59 pp.

INITIAL DISTRIBUTION LIST

		No. Copies
1.	Defense Documentation Center Cameron Station Alexandria, Virginia 22314	2
2.	Library, Code 0142 Naval Postgraduate School Monterey, California 93940	2
3.	Department Chairman, Code 63 Department of Meteorology Naval Postgraduate School Monterey, California 93940	1
4.	Dr. Robert J. Renard, Code 63Rd Department of Meteorology Naval Postgraduate School Monterey, California 93940	8
5.	LT Otto F. McNab 1825 Mehle Avenue Arabi, Louisiana 70032	5
6.	Commanding Officer Fleet Numerical Weather Central Monterey, California 93940	1
7.	Commanding Officer Naval Environmental Prediction Research Facility Monterey, California 93940	1
8.	Department of Meteorology, Code 63 Naval Postgraduate School Monterey, California 93940	1
9.	Department of Oceanography, Code 68 Naval Postgraduate School Monterey, California 93940	1
10.	Director, Naval Oceanography and Meteorology National Space Technology Laboratories Bay St. Louis, Mississippi 39520	1
11.	Mr. Thomas O. Haig Space Science and Engineering Center University of Wisconsin 1225 West Dayton Street Madison, Wisconsin 53706	1

12. LT Carl B. Ihli, USN — 1
U.S. Fleet Weather Central, Guam
Box 12, COMNAVMARIANAS
FPO San Francisco 96630

13. Dr. Glenn H. Jung, Code 63 — 1
Department of Oceanography
Naval Postgraduate School
Monterey, California 93940

14. Dr. Dale F. Leipper, Code 68 — 1
Department of Oceanography
Naval Postgraduate School
Monterey, California 93940

15. Mr. Paul R. Lowe — 1
Naval Environmental Prediction Research Facility
Monterey, California 93940

16. Dr. Alan Weinstein — 1
Naval Environmental Prediction Research Facility
Monterey, California 93940

Thesis
M2575 McNab
c.1
134642
Analysis of statistical parameters derived from satellite digital data (July 1978 GOES-West) for use in diagnosing marine fog areas.